Published in final edited form as:
J Mol Biol. 2013 June 12; 425(11): 1961–1981. doi:10.1016/j.jmb.2013.02.017.

Structural and Functional Studies of γ-Carboxyglutamic Acid Domains of Factor VIIa and Activated Protein C: Role of Magnesium at Physiological Calcium

Kanagasabai Vadivel[1,¶], **Sayeh Agah**[1,¶,δ], **Amanda S. Messer**[1], **Duilio Cascio**[2], **Madhu S. Bajaj**[3], **Sriram Krishnaswamy**[4], **Charles T Esmon**[5], **Kaillathe Padmanabhan**[6], and **S. Paul Bajaj**[1,7,*]

[1]UCLA/Orthopaedic Hospital Department of Orthopaedic Surgery, University of California, Los Angeles, CA 90095, USA

[2]UCLA-DOE Institute for Genomics and Proteomics, Los Angeles, CA 90095, USA

[3]Pulmonology and Critical Care, Department of Medicine, University of California, Los Angeles, CA 90095, USA

[4]Hematology, The Children's Hospital of Philadelphia, Philadelphia, PA 19104, USA

[5]Oklahoma Medical Research Foundation, Howard Hughes Medical Institute, Oklahoma City, OK 73104, USA

[6]Department of Biochemistry and Molecular Biology, Michigan State University, East Lansing, MI 48824, USA

[7]Molecular Biology Institute, University of California, Los Angeles, CA 90095, USA

Abstract

Crystal structures of factor (F) VIIa/soluble (s) tissue factor (TF), obtained under high Mg^{2+} (50 mM Mg^{2+}/5 mM Ca^{2+}), have three of seven Ca^{2+}-sites in the γ-Carboxyglutamic Acid (Gla) domain replaced by Mg^{2+} at positions 1, 4 and 7. We now report structures under low Mg^{2+} (2.5 mM Mg^{2+}/5 mM Ca^{2+}) as well as under high Ca^{2+} (5 mM Mg^{2+}/45 mM Ca^{2+}). Under low Mg^{2+}, four Ca^{2+} and three Mg^{2+} occupy the same positions as in high Mg^{2+} structures. Conversely, under low Mg^{2+}, reexamination of the structure of Gla domain of activated Protein C (APC) complexed with sEPCR has position 4 occupied by Ca^{2+} and positions 1 and 7 by Mg^{2+}. Nonetheless, in direct binding experiments, Mg^{2+} replaced three Ca^{2+}-sites in the unliganded Protein C or APC. Further, the high Ca^{2+}-condition was necessary to replace Mg4 in the FVIIa/sTF structure. In biological studies, Mg^{2+} enhanced phospholipid binding to FVIIa and APC at physiological Ca^{2+}. Additionally, Mg^{2+} potentiated phospholipid-dependent activations of FIX and FX by FVIIa/TF, and inactivation of FVa by APC. Since APC and FVIIa bind to sEPCR involving similar interactions, we conclude that under the low Mg^{2+}-condition, sEPCR binding to

*Address correspondence to: S. Paul Bajaj, 446 Orthopaedic Hospital Research center, 615 Charles E. Young Drive, Los Angeles, CA 90095, USA. Tel: 01-310-825-5622; Fax: 01-310-825-5972; pbajaj@mednet.ucla.edu.
¶These authors contributed equally to this work
δPresent address: Molecular Physiology and Biological Physics, School of Medicine, University of Virginia, Charlottesville, VA 22908, USA

APC-Gla (or FVIIa-Gla) replaces Mg4 by Ca4 with an attendant conformational change in the Gla domain ω-loop. Moreover, since phospholipid and sEPCR bind to FVIIa or APC via the ω-loop, we predict that phospholipid-binding also induces the functional Ca4 conformation in this loop. Cumulatively, the data illustrate that Mg^{2+} and Ca^{2+} act in concert to promote coagulation and anticoagulation.

Keywords

γ-carboxyglutamic acid domains; Ca^{2+} and Mg^{2+} sites; Surface plasmon resonance; Factor VIIa; Activated Protein C

Introduction

The vitamin K-dependent (VKD) plasma proteins are involved in coagulation as well as in anticoagulation. The VKD coagulant proteins include prothrombin and factors VII (FVII), IX (FIX), and X (FX), whereas VKD anticoagulant proteins include Protein C, protein S and protein Z.[1–4] Each VKD protein contains a γ-carboxyglutamic acid (Gla) rich domain at the N-terminus through which it binds to the phospholipid membrane and performs its biological function at the site of injury. The folding of the Gla domain is Ca^{2+}-dependent, which induces conformational changes that transforms this domain from the unfolded non-functional form to the folded functional form.[5–8] However, the concentration of Ca^{2+} required for occupancy of all metal sites in the Gla domain is ≳ 2 mM,[9–13] which exceeds ~1.1 mM physiological concentration present in plasma.[14] Plasma also contains Mg^{2+} at ~0.6 mM (physiological concentration) and its role in augmenting the functions of Gla domains in VKD proteins has generated a renewed interest.[9,12,13,15–21] Here, we further address this issue and provide new insights as to the Ca^{2+}/Mg^{2+} sites in the Gla domains of clotting protein activated FVII (FVIIa) and of anti-clotting protein activated Protein C (APC).

During coagulation, FVIIa in association with its cofactor, tissue factor (TF), converts FIX to FIXa and FX to FXa.[2] Previous structures of FVIIa in complex with soluble (s) TF were obtained either in the presence of Ca^{2+} only† (10 mM Ca^{2+})[22] or in high concentrations (50 mM) of Mg^{2+} at 5 mM Ca^{2+} (high Mg/low Ca condition).[12] In the presence of Ca^{2+} only, all seven metal sites‡ in the Gla domain are occupied by Ca^{2+}. Under the high Mg/low Ca condition (50 mM Mg^{2+}/5 mM Ca^{2+}), metal positions 1, 4 and 7 are occupied by Mg^{2+} and the remaining four by Ca^{2+}. In contrast, under a low Mg/low Ca condition (2 mM Mg^{2+}/5 mM Ca^{2+}), the Gla domain of FIX bound to FIX-binding protein (FIX-bp) has metal positions 1 and 7 occupied by Mg^{2+} and position 4 occupied by Ca^{2+}.[17] Two possibilities

†crystallization conditions are defined as follows: Ca^{2+} only, 100 mM cacodylate, pH 5.0, 10 mM $CaCl_2$ and 20% PEG 4000; high Mg/low Ca, 50 mM Tris-HCl, pH 7.0, 5 mM $CaCl_2$, 50 mM $MgCl_2$, 150 mM NaCl, and 20% PEG 4000 for FVIIa/sTF; low Mg/low Ca, 50 mM Tris-HCl, pH 7.0, 5 mM $CaCl_2$, 2.5 mM $MgCl_2$, 150 mM NaCl, and 20% PEG 4000 for FVIIa/sTF; 50mM HEPES, pH 7.0, 5 mM $CaCl_2$, 5 mM $MgCl_2$, 100 mM KCl and 5% (v/v) PEG 400 for APC-Gla/sEPCR; 30 mM Tris-HCl, pH 8.0, 5mM $CaCl_2$, 2 mM $MgCl_2$,14% PEG 6000 for FIX-Gla/FIX-bp; low Mg/high Ca, 50 mM Tris-HCl, pH 7.0, 45 mM $CaCl_2$, 5 mM $MgCl_2$, 150 mM NaCl, and 20% PEG 4000 for FVIIa/sTF.

‡The metals in the Gla domain are numbered 1–7 according to the system of Tulinsky and co-workers (5), who first described the structure of the Gla domain of prothrombin fragment 1. The Gla domain of FIX has an additional metal binding site (number 8) coordinated to Gla36 and Gla40 in FIX residue numbering.

exist as to the reasons for position 4 to be occupied by Mg^{2+} in the FVIIa/sTF structure[12] and by Ca^{2+} in the FIX-Gla structure.[17] One, the Mg^{2+} concentration used in FVIIa/sTF crystallization experiments was extremely high[12], whereas it was low in the FIX-Gla domain crystallization protocols.[17] Two, the FIX-Gla domain via its ω-loop is bound to FIX-bp in the crystal structure,[17] whereas it is unliganded in the FVIIa/sTF structure.[12] Thus, FVIIa/sTF structures under a low Mg/low Ca condition would be useful in understanding the specificity of the metal site at position 4 and its contribution to the conformation of the ω-loop in Gla domains. Further, it would be important to determine whether high concentrations of Ca^{2+} can displace Mg^{2+} at position 1, 4 or 7. Towards attaining these goals, we now report structures[‖] of FVIIa/sTF under a low Mg/low Ca condition (2.5 mM Mg^{2+}/5 mM Ca^{2+}) at 1.72 Å as well as under a low Mg/high Ca condition (5 mM Mg^{2+} /45 mM Ca^{2+}) at 1.80 Å. Moreover, in the new FVIIa/sTF structure under low Mg/low Ca condition, the sTF 159–166 residue loop is ordered and provides new insight for its role in substrate/inhibitor interactions. In this context, we address the role of FVIIa residue Arg36, and of sTF residues Lys159 and Lys165/Lys166 implicated in substrate/inhibitor recognition.[23–26]

Earlier, under a low Mg/low Ca condition (5mM Mg^{2+}/5 mM Ca^{2+}), the Gla domain of Protein C bound to soluble endothelial Protein C receptor (sEPCR) has been reported to contain all seven metal binding sites occupied by Ca^{2+}.[27] In light of the FVIIa/sTF[12] and FIX-Gla[17] structures, we reexamined the structure of the APC-Gla/sEPCR complex[27] to determine whether any of the seven Ca^{2+} sites in the Gla domain are occupied by Mg^{2+}. To substantiate our findings, we performed direct Ca^{2+}-binding studies to ascertain the number of Ca^{2+}-sites present in the Gla domains of wild-type (WT) Protein C, D71K/E225K Protein C and APC in the presence or absence of physiological Mg^{2+}. These crystallographic and metal binding studies, which elucidate the numbers and positions of Ca^{2+}/Mg^{2+} sites in the Gla domains of FVIIa and Protein C/APC under different conditions are presented in the first part of the paper. We also discuss the specific site occupancy by Mg^{2+} and Ca^{2+} based upon their hard and soft characteristics as it relates to their charge densities and polarizabilties.[28,29]

VKD proteins via their Gla domains bind to phosphatidylcholine (PC)/phosphatidylserine (PS) synthetic vesicles as well as to cell membranes that have exposed PS.[30,31] The role of Ca^{2+} to promote phospholipid binding has been extensively studied,[32–35] whereas the contribution of Mg^{2+} in this process is poorly understood.[36] Here, we investigate the effect of physiological concentrations of Mg^{2+} in augmenting the Ca^{2+}-dependent binding of FVIIa and APC to PC/PS phospholipid bilayer using surface plasmon resonance (SPR). We also study the effect of physiological Mg^{2+} in promoting the activation of FX and FIX by FVIIa bound to TF on the activated human peripheral blood monocytes as well as in the microparticles. Finally, we study the effect of Mg^{2+} on the phospholipid-dependent inactivation of activated factor V (FVa) by APC. These biochemical studies and their physiological implications are presented in the second part of the paper.

[‖]The atomic coordinates and structure factors (code 3TH2, 3TH3, 3TH4 and 3JTC) have been deposited in the Protein Data Bank, Research Collaboratory for Structural Bioinformatics, Rutgers University, New Brunswick, NJ (http:/www.pdb.org).

Results

Part I: Structural studies

Overall, the structures of the FVIIa/sTF complexes obtained under different concentrations of Ca^{2+}/Mg^{2+} are similar except variations in their Gla domain ω-loops (Fig. 1). In these complexes, the ω-loop adopts two different conformations, which arise from variations in the number of Ca^{2+} and Mg^{2+} bound to the FVIIa-Gla domain and their coordination geometries. Data processing and the structure refinement statistics of all structures are provided in Table 1 under Materials and Methods Section.

Occupancy of Ca^{2+} and Mg^{2+} in FVIIa/sTF structures under the low Mg/low Ca (2.5 mM Mg^{2+}/5 mM Ca^{2+}) and under low Mg/high Ca (5 mM Mg^{2+}/45 mM Ca^{2+}) condition—In previous structures under the high Mg/low Ca (50 mM Mg^{2+}/5 mM Ca^{2+}) condition, metal positions 1, 4 and 7 are occupied by Mg^{2+} in the Gla domain of FVIIa/sTF (2A2Q).[12] To determine whether position 4 is occupied by Ca^{2+} under a low Mg/low Ca condition, as is the case with FIX-Gla/FIX-bp complex, we obtained crystals of benzamidine-VIIa/sTF under 2.5 mM Mg^{2+}/5 mM Ca^{2+} (1.72 Å, R_{work} 18.4; R_{free} 22.9). Unlike in FIX-Gla/FIX-bp complex, in the FVIIa/sTF structure (3TH2, Fig. 1), metal positions 1, 4 and 7 are occupied by Mg^{2+} and the ω-loop fold is similar to 2A2Q.[12] In additional experiments, when concentrations of Mg^{2+}/Ca^{2+} was further reduced to 1.25 mM Mg^{2+}/2.5 mM Ca^{2+}, dansyl-Glu-Gly-Arg (dEGR)-VIIa/sTF yielded crystals (2.7 Å) in which the Gla domain is disordered. This structure is similar to the reported sTF/FVIIa protease domain mutant structure obtained in citrate, where the Gla domain is also disordered.[38] This is most probably due to the additions of salts, precipitants and additives used for crystallization that might affect the cation concentrations in the crystallization drops in the present study and in the study of Bjelke *et al*[38]. Thus, a new set of conditions will be necessary to obtain FVIIa/sTF crystals under physiological Mg^{2+}/Ca^{2+}, in which the Gla domain is ordered.

Next, we investigated whether the low Mg/high Ca (5 mM Mg^{2+}/45 mM Ca^{2+}) condition would yield the FVIIa Gla domain in which one or more of the three Mg^{2+}-sites are occupied by Ca^{2+}. Under the low Mg/high Ca condition, the folding of the ω-loop in dEGR-VIIa/sTF (1.8 Å) is similar to the Ca^{2+} only 1DAN structure,[22] but positions 1 and 7 are still occupied by Mg^{2+} (3TH4, Fig. 1). Thus, only site 4 is switched from Mg^{2+} to Ca^{2+} under the low Mg/high Ca condition. The different conformations of the ω-loop under occupancy of position 4 by Ca^{2+} (Ca4 conformer, 3TH4) versus Mg^{2+} (Mg4 conformer, 3TH2) is shown in the expanded view of Fig. 1. The coordination geometries of Mg^{2+} at position 1 and 7 under the low Mg/high Ca condition are shown in Figs. 2A and 2B. The coordination geometries for Ca^{2+} and Mg^{2+} at position 4 under the low Mg/high Ca condition and under the low Mg/high Ca condition are shown in Fig.2C and 2D, respectively. Note that in the low Mg/low Ca condition, the Mg^{2+} at position 4 is coordinated to Gla16, Gla26 and two water molecules, whereas in low Mg/high Ca, the Ca^{2+} at position 4 is coordinated to Ala1, Asn2, Gla6, Gla7, Gla16 and Gla26.

Functional role of Arg36 in FVIIa, and of Lys159 and Lys165 in sTF—Arg36 in FVIIa,[23] and Lys159[24] and Lys165[24,26] in TF have been implicated in macromolecular substrate FX as well as in tissue factor pathway inhibitor (TFPI) recognition.[25] Since the TF 159–165 loop in previous FVIIa/sTF structures[12,22] is disordered, its location and interactions with the neighboring residues are not known with certainty. However, the 159–165 residues of sTF are well ordered in the new low Mg/low Ca structure (Fig. 3). Arg36 of FVIIa makes an extensive network of hydrogen bonds with sTF residues 159–164 (Fig. 3A). Similarly, Lys159 makes bifurcated hydrogen bonds with Asp180 and Glu183 of sTF (Fig. 3B), and the carboxyl group of Gla35 could possibly make a salt bridge with the side chain NH_2 of Lys165 (Fig. 3C). However, since the side chain of Lys165 of sTF is disordered, it is possible that water occupies the site where the side chain ε-amino group is positioned. Overall, it appears that the proposed residues will need to dissociate from the existing interactions prior to binding to FX or TFPI.

Occupancy of Ca^{2+} and Mg^{2+} in the APC-Gla/sEPCR structure under the low Mg/low Ca condition—The structure of APC-Gla/sEPCR complex (1LQV) is reported with seven Ca^{2+} bound in the APC-Gla domain despite the presence of 5 mM Mg^{2+} in the crystallization drop. Additionally, the APC-Gla domain is involved in EPCR binding, which is dependent on Ca^{2+} and enhanced by Mg^{2+}.[39] Based upon these observations coupled with the finding of Mg^{2+} sites in the Gla domains of FVIIa and FIX, we postulate that the Gla domain in the APC-Gla/sEPCR structure should have certain metal sites occupied by Mg^{2+}. Thus, we reexamined the APC-Gla/sEPCR structure and found that the Ca^{2+} at positions 1 and 7 in the APC-Gla domain were refined with partial occupancy. When Ca^{2+} at positions 1 and 7 were refined with full occupancy, negative electron density was observed in the difference map ($F_{obs} - F_{calc}$) surrounding these metal ions (Fig. 4A, left and Fig. 4C, left). Refining the structure with Mg^{2+} at position 1 and 7 eliminated the negative density in the difference ($F_{obs} - F_{calc}$) map (Fig. 4A, right and Fig4C, right). Further, refining the structure with Mg^{2+} at position 4 revealed a positive density in the difference map, which indicates that position 4 is occupied by Ca^{2+} (Fig. 4B).

Comparison of the atomic temperature factors (B-values) of Ca^{2+}/Mg^{2+} with that of surrounding residues can yield information as to the type of metal at a given site. Accordingly, when metal positions in APC-Gla were refined as Ca^{2+}, the B-values were 24.7 $Å^2$, 15.1 $Å^2$ and 42.9 $Å^2$ for sites 1, 4 and 7, respectively; refinement of these sites with Mg^{2+} yielded the corresponding B-values of 15.8 $Å^2$, 9.5 $Å^2$, and 33.3 $Å^2$. The average B-values of the atoms coordinating the metals at sites 1, 4 and 7 were 15.9 $Å^2$, 15.4 $Å^2$ and 31.3 $Å^2$, respectively. Noticeably, the B-values for sites 1 and 7 for Mg^{2+} are similar to the average B-values for coordinating residues, whereas they are higher for Ca^{2+}. In contrast, the B-value for site 4 for Mg^{2+} is lower than the coordinating residues, whereas it is similar for Ca^{2+}. Thus, the temperature factor analysis indicate that in APC-Gla, sites 1 and 7 are occupied by $Mg^{2+}$and site 4 is occupied by Ca^{2+}. This finding is in consistent with the position 4 occupied by Ca^{2+} in FIX-Gla/FIX-bp complex but is in contrast to the position 4 occupied by Mg^{2+} in FVIIa-Gla domain under the low Mg/low Ca condition.

Yang and Pflugrath[40] demonstrated that the anomalous signal from Ca^{2+} can be used to determine the phases if the dataset has high redundancy (≥10) and is collected at the Cu *K*α

wavelength. Since the dataset for APC-Gla/sEPCR was collected in-house at 1.54 Å, we calculated the anomalous map to unambiguously identify the Ca^{2+}-sites in the APC-Gla domain. The resultant anomalous map obtained for APC-Gla/sEPCR is shown in Fig. 4D. The metal at sites 2 to 5 gave strong anomalous signals for Ca^{2+}, whereas the metal at site 6 gave a very weak signal. Although the anomalous signal is weak for the metal at site 6, the distances with the coordinating atoms and the atomic temperature factors of the environment indicate that this site is occupied by Ca^{2+}. As expected, we did not observe an anomalous signal either at metal position 1 or 7. Collectively, the anomalous signals observed confirm that in the APC-Gla, the sites 1 and 7 are occupied by Mg^{2+} and the remaining five by Ca^{2+}.

$^{45}Ca^{2+}$-binding to dEGR-APC, decarboxylated dEGR-APC, WT-Protein C and D71K/E225K Protein C by equilibrium dialysis—Previous studies have suggested that the Gla domain of human Protein C/APC contains a number of high and low affinity Ca^{2+}-binding sites.[11,41] Further, two of the high affinity Ca^{2+} sites are located in the non-Gla region of the protein.[42] Here, we determined the number of Ca^{2+}-binding sites present in the APC-Gla domain in the presence and absence of physiological Mg^{2+}. These data are presented in Fig. 5A. In the absence of Mg^{2+}, full-length dEGR-APC bound nine (K_d ~400 μM after completion of positive cooperativity), and decarboxylated dEGR-APC bound two Ca^{2+} ions. The two Ca^{2+}-binding sites present in the EGF1 and the protease domain of decarboxylated APC could not be displaced by Mg^{2+} (Fig. 5, *Inset*). In full-length APC, Mg^{2+} displaced a maximum of 3 Ca^{2+} sites at 5 mM Ca^{2+} and 0.6 mM Mg^{2+} (Fig. 5A and Fig. 5A *Inset*, closed circles). The K_d for the six sites (four in the Gla domain) after completion of the positive cooperativity is ~100 μM. In further experiments, D71K/E225K Protein C bound seven Ca^{2+} ions (K_d ~350 μM) in the absence (Fig. 5B, open circles) and four Ca^{2+} ions (K_d ~100μM) in the presence of 0.6 mM Mg^{2+} (Fig. 5B, closed circles). Mg^{2+} displaced 3 Ca^{2+} ions in WT-Protein C (Fig. 5B *Inset*, closed circles) or D71K/E225K Protein C (Fig. 5B *Inset*, open circles). From these data, we conclude that as in FVIIa, Mg^{2+} occupies three sites at positions 1, 4 and 7 in the unliganded Gla domain of Protein C or APC at plasma concentrations of Ca^{2+}/Mg^{2+}.

Part II: Biochemical studies

In the previous section, we defined the specific Mg^{2+}-sites in the Gla domains of FVIIa and Protein C/APC under different conditions. In this section, we explore the role of Mg^{2+} in promoting phospholipid binding and its functional consequence. We first provide data on FVIIa followed by studies with APC.

Contribution of Mg^{2+} to binding of FVIIa to phospholipid and activations of FX and FIX on lipopolysaccharide (LPS)-stimulated peripheral blood monocytes —We used SPR to study the role of Mg^{2+} on binding of D-Phe-Phe-Arg (DFFR)-VIIa to the PC/PS bilayer. These data are presented in Fig. 6A–C and summarized in Table 2. These data indicate that the k_{on} is ~2-fold improved under physiological Ca^{2+}/Mg^{2+} as compared to physiological Ca^{2+} only; however the k_{off} values are similar in all cases. In further experiments, we studied the effect of Mg^{2+} on the Ca^{2+}-dependence of D-FFR-VIIa binding to the PC/PS bilayer. These data are presented in Fig. 6D. In these experiments, a constant concentration (800 nM) of D-FFR-FVIIa was used and the response units (RU, a measure of

phospholipid binding) values were obtained at different concentrations of Ca^{2+} in the presence or absence of physiological Mg^{2+}. In the absence of Mg^{2+}, D-FFR-VIIa required > 0.5 mM Ca^{2+} to depict noticeable binding to phospholipid (Fig. 6D, open circles). This Ca^{2+} requirement was most diminished at physiological concentrations of Mg^{2+} (Fig. 6D, closed circles). Further, binding of phospholipid to D-FFR-VIIa reached a plateau value at ~2 mM Ca^{2+} in the absence of Mg^{2+}, whereas it reached a plateau value at physiological Ca^{2+}/Mg^{2+}. However, Mg^{2+} did not enhance PC/PS binding to D-FFR-VIIa at saturating concentrations of Ca^{2+}.

Previously, Mg^{2+} has been shown to potentiate the activation of FX by FVIIa/TF assembled on synthetic phospholipid vesicles.[12,20] Here, we examined whether physiological Mg^{2+} potentiates activation of FX as well as of FIX by FVIIa/TF assembled on the activated monocyte surface or microparticles. As depicted in Fig. 7A, 1 nM FVIIa/TF assembled on the monocyte surface (10^6/ml) activated FX (100 nM) at 0.8 nM/min in the presence of 1.1 mM Ca^{2+}; 2.4 nM/min at 1.7 mM Ca^{2+}; and 3.5 nM/min at physiological Ca^{2+}/Mg^{2+} or at 5 mM Ca^{2+}. Similarly, plasma concentrations of Mg^{2+} also enhanced the rate of activation of ^{3}H-FIX (100 nM) at physiological Ca^{2+} (Fig. 7B). Next, we examined the effect of Mg^{2+} on the activations of FX and FIX using TF bearing microparticles. These data are presented in Table 3. Cumulatively, our data indicate that in both systems (cells or microparticles), plasma concentrations of Mg^{2+} potentiates the activation of FX or FIX ~4 fold at physiological concentration of Ca^{2+}.

Contribution of Mg^{2+} to binding of APC to phospholipid and inactivation of FVa—We used SPR and a similar approach as outlined earlier for FVIIa (Fig. 6) to study the effect of Mg^{2+} on binding of dEGR-APC to the PC/PS bilayer. These data are presented in Fig. 8A–C and Table 4. Similar to the data for FVIIa (Fig. 6), the APC data also indicate that the k_{on} for binding of PC/PS to APC is significantly improved (~4-fold) under physiological Ca^{2+}/Mg^{2+} as compared to physiological Ca^{2+} only; however, the k_{off} values are similar in all cases. In additional experiments, we studied the effect of Mg^{2+} on the Ca^{2+}-dependence of dEGR-APC binding to the PC/PS bilayer. As in D-FFR-VIIa, a constant concentration (800 nM) of dEGR-APC was used and the RU values were obtained at different concentrations of Ca^{2+} in the presence or absence of physiological Mg^{2+}. Binding of APC reached saturation at ~1 mM Ca^{2+} in the presence of physiological Mg^{2+}, whereas ~2 mM Ca^{2+} was required to reach saturation in the absence of Mg^{2+} (Fig. 8D). However, Mg^{2+} did not enhance PC/PS binding to dEGR-APC at saturating concentrations of Ca^{2+}.

In previous studies, incorporation of phosphatidylethanolamine (PE) into the phospholipid vesicles has been shown to enhance the rate of inactivation of FVa by APC.[43] Hence, we studied the effect of Mg^{2+} on the inactivation of FVa using PE/PC/PS vesicles. The data using varying concentrations of Ca^{2+} in the presence or absence of physiological concentrations of Mg^{2+} are presented in Fig. 9. In the absence of Mg^{2+}, ~50% loss of FVa activity at 0.5 mM Ca^{2+} (Fig. 9A, open circles) or 0.8 mM Ca^{2+} (Fig. 9B, open circles) occurs in ~45 seconds. At physiological concentration of 1.1 mM Ca^{2+}, ~50% loss of FVa activity occurs in ~30 seconds (Fig. 9C, open circles). Addition of 0.6 mM Mg^{2+} to each of these three conditions reduces the ~50% FVa inactivation time to ~15 seconds (Figs. 9A–9C, closed circles). However, addition of 0.6 mM physiologic Mg^{2+} to 2 mM Ca^{2+} had no

further effect on the FVa inactivation rate (Fig. 9D). Thus, Mg^{2+} exerts its effect only up to physiological concentrations of 1.1 mM Ca^{2+} in inactivating FVa by APC.

Discussion

Metal ion specificity in the Gla domains of circulating VKD proteins

Our laboratory is interested in delineating the distribution and function of Ca^{2+} and Mg^{2+} ions in the Gla domains of VKD proteins. From the crystal structure data and Ca^{2+}-binding studies, it appears that four Ca^{2+} and three Mg^{2+} are bound to the Gla domain of circulating FVII/FVIIa. Direct Ca^{2+}-binding data also indicate that prothrombin fragment 1,[9,12] Protein C and APC (Fig. 5) each has four Ca^{2+} and three Mg^{2+} ions bound to its Gla domain at physiological Ca^{2+}/Mg^{2+}. However, in direct binding assays, the Gla domain of human FIX binds four Ca^{2+} and four Mg^{2+} under physiological Ca^{2+}/Mg^{2+}.[13] The additional Mg^{2+}-binding site in the FIX-Gla domain involves Gla36 and Gla40 and is at position 8;[17] this site is absent in FVII,[12] prothrombin fragment 1,[5,35] Protein C/APC.[27] For clarification, a multiple sequence alignment of Gla domains of VKD proteins and the residues coordinating to Ca^{2+} and Mg^{2+} under different concentrations of Ca^{2+}/Mg^{2+} is given in supplement Fig. S1. Based upon these observations, we postulate that Gla domain of each circulating VKD protein has four Ca^{2+} ions bound at positions 2, 3, 5 and 6, and the remaining divalent metal binding sites including 1, 4 and 7 are occupied by Mg^{2+}.

Under the low Mg/high Ca (5 mM Mg^{2+}/45 mM Ca^{2+}) condition, position 4 in the Gla domain of FVIIa is occupied by Ca^{2+}. It should be noted that even at 5 mM Mg^{2+}/20 mM Ca^{2+}, position 4 is occupied by Mg^{2+}.§ It is only under 5 mM Mg^{2+}/45mM Ca^{2+} that site 4 is occupied by Ca^{2+} (Fig. 1). Thus very high concentrations of Ca^{2+} are needed to switch Mg4 to Ca4 in the unliganded Gla domain of FVIIa. For comparison, the coordination of each metal when Mg^{2+} or Ca^{2+} occupies position 4 is shown in Fig. 10A and Fig. 10B, respectively. Importantly, as compared to previously reported structures of FVIIa/sTF, all metal ions in the low Mg/high Ca structure (3TH4) possess complete coordination, including four additional ligands for metal position 6, two for metal position 1, and one for metal position 7 (Fig.10B, Table S1). It should be noted that in the low Mg/low Ca structure, Gla6 interacts with Ca6 through a water molecule; and Gla7 interacts with Mg4 through two water molecules (Fig. 10A). In contrast, in the low Mg/high Ca structure, Gla6 now directly interacts with Ca4 and Ca5 and not with Ca6; and Gla7 directly interacts with Ca2, Ca3 and Ca4 (Fig. 10B). Consequently, there are four water molecules that are expelled from the space between the ω-loop and the two helices, namely helix 12–17 and helix 23–32 of FVIIa (Figs. 10A and 10B). This has important biological implications outlined below.

§We also obtained crystals of benzamidine-VIIa/sTF under 5 mM Mg^{2+}/20 mM Ca^{2+} (2.5 Å, R_{work} 18.7; R_{free} 24.3), 5 mM Mg^{2+}/10 mM Ca^{2+} (2.2 Å, R_{work} 19.4; R_{free} 23.8). In these two structures, the fold of the ω-loop is similar to 2A2Q[12] as well as to the low Mg/low Ca condition (2.5 mM Mg^{2+}/5 mM Ca^{2+}) 3TH2 structure presented here. Further, the metal sites at position 1, 4, and 7 are occupied by Mg^{2+} in all of the three structures.

Hardness of Mg^{2+} versus Ca^{2+} dictates position 4 metal ion specificity under different conditions

In the low Mg/low Ca condition, position 4 in the Gla domain of FVIIa/sTF is occupied by Mg^{2+} (Mg4 conformer), whereas in the low Mg/high Ca condition, it is occupied by Ca^{2+} (Ca4 conformer). However, under the low Mg/low Ca condition, site 4 is occupied by Ca^{2+} in the APC-Gla/sEPCR or FIX-Gla/FIX-bp structure.[17] The interactions between the APC-Gla/sEPCR complex and FIX-Gla/FIX-bp complex are shown in Fig. 10C and Fig. 10D, respectively. Hydrophobic contacts, hydrogen bonds and ionic interactions are observed between APC-Gla and sEPCR or FIX-Gla and FIX-bp. Since ω-loop of the Gla domain is involved in binding, the hydrophobic contacts appear to dominate the interactions in these complexes. Such interactions might induce a conformational change in the ω-loop of the APC-Gla or FIX-Gla from Mg4 conformer to the Ca4 conformer with a concomitant binding of Ca^{2+} at position 4.

Does phospholipid binding to the ω-loop also induce a similar conformational transition? Three models of interaction of phospholipid with Gla domains have been described.[30,35,44] In the first two models, the ω-loop is not buried in the membrane[43] or only the keel is inserted.[35] In the third model obtained by molecular dynamics simulations, the ω-loop reaches and stays at the acyl chain layer.[30] Primarily, these models suggest that the hydrophobic residues present in the ω-loop interact with membrane acyl chains while the bound Ca^{2+} ions and positively charged residues interact with the negatively charged carboxyl/phosphate groups of phospholipid. From these molecular dynamics simulations, it follows that the Gla-domain/phospholipid interactions have many similarities observed for APC-Gla/sEPCR or FIX-Gla/FIX-bp interactions: 1) hydrophobic interactions in all cases are similar; 2) Ca4 and Ca5 do not directly interact either with phospholipid or sEPCR and FIX-bp; and 3) Ca1/Mg1 and Ca2 make ionic interactions with sEPCR,[27] FIX-bp[17] or phospholipid.[30] Another observation to note here is that the Gla domain of FVIIa also binds to sEPCR,[45] and that phospholipid and sEPCR compete for binding to the APC-Gla domain.[39] Similarly, phospholipid and FIX-bp are thought to compete for binding to the FIX-Gla domain.[17,21] Further, the interactions observed between FVIIa-Gla domain and phospholipid are in the Ca4 conformer of the ω-loop.[30] Thus, it is conceivable that phospholipid binding might also induce a conformational change in the ω-loop from the Mg4 conformer (Fig. 10A) to the Ca4 conformer (Fig. 10B).

The concept that phospholipid binding to the ω-loop of VKD proteins replaces Mg^{2+} at site 4 by Ca^{2+} is supported by metal ion binding selectivity studies using the subvalence concept.[29] Mg^{2+} is a hard metal ion, which has a high valence electron charge density and is weakly polarizable.[28,46] In comparison, Ca^{2+} is relatively a soft metal ion, which has a lower valence electron charge density and is polarizable.[28] Further, Mg^{2+} binds to its ligands primarily via electrostatic interactions, whereas Ca^{2+} binds to its ligands via electrostatic and partial covalent bonds.[28,29] Moreover, the lifetime of water molecules associated in the first solvation shell of Mg^{2+} is on the order of hundreds of picoseconds, as compared to only a few picoseconds for Ca^{2+}.[47] In support of these Ca^{2+}/Mg^{2+} metal ion characteristics, both the experimental data and the theoretical calculations reveal that Mg^{2+} occupies only one central (site 4) and each of the external metal sites in the Gla domains[12,29] (present study).

In the Mg4 conformation, the space between the ω-loop and the two helices (composed of FVIIa residue 12 to 17 and 23 to 32) is occupied by several water molecules (Fig. 10A). Such is predicted to be the case for APC and FIX as well. Binding of biological ligands such as EPCR[27] or FIX-bp[17] and predictably phospholipid[30] shifts the ω-loop towards the two helices that lead to the expulsion of inner water molecules (Figs. 10C and 10D). The protruding nonpolar residues of the ω-loop are now embedded in the hydrophobic environment,[17,27,30] which favors occupancy of site 4 by Ca^{2+} (Figs. 10C and 10D). Now, Gla6 and Gla7 directly interact with Ca2, Ca3, Ca4, and Ca5 (Figs. 10A–D). This is consistent with the protein crystal structure database that Ca^{2+} ions bind fewer water molecules than Mg^{2+}.[48] However, one should note that the proposed mechanism for switching from Mg4 to Ca4 conformer with a concomitant binding of Ca^{2+} at site 4 is only speculative at this point.

Functional significance of Mg^{2+} sites in VKD proteins

Mg^{2+} augments phospholipid binding to FVIIa and APC at the physiological concentration of 1.1 mM Ca^{2+} (Figs. 6 and 8). Our K_d values for interaction of phospholipid at saturating concentrations of Ca^{2+} for FVIIa and APC agree well with the previous reports.[49,50] Earlier, Mg^{2+} has been shown to accelerate synthetic phospholipid-dependent coagulation reactions involving FVII,[12] FIX,[13,15,16,51] FX[20] and prothrombin.[9] Here, we show that Mg^{2+} similarly accelerates Ca^{2+}-dependent activations of FX and FIX by FVIIa/TF assembled on biological membranes (Fig. 7). Our data also reveal that Mg^{2+} potentiates phospholipid-dependent inactivation of FVa by APC at physiological Ca^{2+} (Fig. 9). Cumulatively, the data indicate that Mg^{2+} potentiates each coagulation and anticoagulation reaction involving VKD proteins at physiological Ca^{2+}.

Implications for interactions of FVIIa-Arg36, and sTF-Lys159/Lys165 in FVIIa/sTF structure

As pointed out earlier, Arg36 of FVIIa and Lys159 and Lys165 of TF are proposed to be involved in macromolecular substrate/inhibitor recognition.[23–26] However, side chains of these amino acids make extensive ionic and hydrogen bond interactions with the neighboring residues in the FVIIa/sTF complex (Fig. 3). For these residues to be involved in macromolecular substrate or TFPI recognition, several existing interactions in the FVIIa/sTF complex will need to be unlocked, a process that might be energetically unfavorable. Further, Pedersen and associates[52] have proposed that either Lys165 or Lys166 (but not both) of TF may be involved in FXa and/or TFPI recognition. From the crystal data, it appears that Lys166 is a plausible candidate for this interaction. Experimentally determined structures of the ternary complex of FVIIa/sTF/FX(Xa) and/or the quaternary complex of FVIIa/sTF/Xa/TFPI are needed to resolve these issues.

Materials and Methods

Reagents

Magnesium chloride, Calcium chloride, and PEG 4000 were purchased from Hampton Research, Laguna Niguel, CA. NaB^3H_4 (100 mCi) and $^{45}CaCl_2$ (1 mCi) were purchased from PerkinElmer, Shelton, CT. PE, PS and PC were obtained from Avanti Polar Lipids, Inc., Alabaster, AL. D-FFR-ck and dEGR-ck were obtained from Calbiochem-Novabiochem

Corporation, La Jolla, CA. FV deficient plasma was from George King Bio-Medical, Inc., Overland Park, KS. Ficoll-Hypaque was obtained from Pharmacia, LKB biotechnology, Piscataway, NJ. The chromogenic substrate S-2222 (*N*-Benzoyl-L-isoleucyl-L-glutamyl-glycyl-L-arginine-*p*-nitroaniline) was obtained from Diapharma, Columbus, OH. Escherchia coli serotype 0127:B8 bacterial LPS, Percoll, Trizma (Tris base) and benzamidine were obtained from Sigma-Aldrich Inc., St Louis, MO.

Isolation of monocytes and cell derived microparticles containing TF

Protocols for obtaining human blood were approved by the institutional review board and informed consent was obtained from participants. Monocytes were isolated from heparinized venous blood drawn from healthy donors as described previously.[53] The preparation contained 90–95% monocytes as identified by the non-specific esterase activity,[54] with 95% viability using the Trypan Blue exclusion method.[55] Monocytes were cultured at 37 °C with 5% CO_2 using RPMI-1640 medium containing 15% fetal calf serum. For LPS stimulation, monocytes were cultured non-adherently in plastic dishes with 1 μg/ml LPS with constant rocking to prevent adhesion and aggregation. Endotoxin contamination in buffers and media using the Limulus Amebocyte Lysate assay was <40 pg/ml.

Microparticles were obtained from the conditioned media as described.[56] Briefly, the media was centrifuged at 1000×g for 5 min to remove cell debris followed by centrifugation at 16,000×g for 2.5 h to yield pellet containing microparticles. The pellet was suspended in 0.05 M Tris/0.15 M NaCl (TBS), pH 7.4 with the starting volume of media and centrifuged again at 16,000×g for 2.5 h to remove any soluble contaminants. The pellet was then suspended in TBS, pH 7.4 at 4 °C and used within 2 days for FX and ^{3}H-FIX activation measurements.

Proteins

Human FVIIa and sTF were obtained as described previously.[12] FIX and FX were purified from human plasma as outlined.[57] Human APC was obtained from Hematologic Technologies, Inc., Essex Junction, VT. [^{3}H]Sialyl-FIX (~3×10^8 cpm/mg) was prepared by the general technique of Van Lenten and Ashwell[58] as previously described.[59] Human FVa was obtained as described.[60] dEGR-VIIa, D-FFR-VIIa, and dEGR-APC were prepared and the unbound inhibitor in each case was removed as outlined earlier.[61] Decarboxylated dEGR-APC was prepared by thermal decarboxylation of Gla residues as described for prothrombin.[62] Wild-type human Protein C was expressed in embryonic kidney 293 cells as described for the hybrid factor IX protein containing the Gla and EGF1 domains of Protein C.[63] For expression of D71K/E225K Protein C, the codon AAG was substituted for codon GAC corresponding to Asp71, as well as for the codon GAG corresponding to Glu225 (Glu70 in chymotrypsin numbering) in human Protein C cDNA[64] by site directed mutagenesis. The D71K/E225K Protein C, which is predicted to lack EGF1 domain[65] and the protease domain[66] Ca^{2+}-binding sites was expressed in kidney 293 cells as described. Both WT-Protein C and D71K/E225K Protein C were purified as outlined.[63] All proteins were ~98% pure and contained the appropriate subunits as analyzed by SDS-PAGE using the Laemmli buffer system.[67]

Crystallization

Benzamidine-VIIa/sTF and dEGR-VIIa/sTF complexes were crystallized using the previously described conditions[12] except varying concentrations of Ca^{2+} and Mg^{2+} were used. Ca^{2+} concentrations varied from 2.5 mM to 45 mM, and the Mg^{2+} concentrations varied from 1.25 mM to 5 mM. The PEG 4000 concentration used was 16–22%. Crystals appeared within four to six months and were flash frozen without additional cryoprotectant.

X-ray data collection

All data sets were collected at Advanced Light Source, Berkeley using the beam line 8.2.1. Complete data sets were collected for five crystals obtained under different Ca^{2+} and Mg^{2+} concentrations. These are: one crystal (benzamidine-VIIa/sTF) that diffracted to 1.72 Å under low Mg/low Ca condition; a second crystal (benzamidine-VIIa/sTF) that diffracted to 2.5 Å under 5 mM Mg^{2+}/10 mM Ca^{2+}; a third crystal (benzamidine-VIIa/sTF) that diffracted to 2.2 Å under 5 mM Mg^{2+}/20 mM Ca^{2+}; a fourth crystal (dEGR-VIIa/sTF) that diffracted to 1.80 Å under low Mg/high Ca; and a fifth crystal (dEGR-VIIa/sTF) that diffracted to 2.7 Å under 1.25 Mg^{2+}/2.5 mM Ca^{2+}, a condition under which the Gla domain is disordered. The first four crystals belong to the orthorhombic space group $P2_12_12_1$ with one molecule in the asymmetric unit. The fifth crystal in which the Gla domain is disordered belongs to the orthorhombic space group $P2_1$ with one molecule in the asymmetric unit. Autoindexing, integration and scaling of data were performed using HKL2000 suite.[68]

Structure determination and refinement

The initial phases of the first four crystals, which belong to the space group $P2_12_12_1$, were obtained using the previous FVIIa/sTF isomorphous structures (PDB codes 2A2Q and 1DAN) as the starting models.[12,22] Since the fifth crystal (dEGR-FVIIa/sTF complex) crystallized in a different space group, it was solved by molecular replacement using AMoRe[69] with 2A2Q as the starting model. The protein residues were fitted using the program COOT.[70] The refinement was carried out using REFMAC[71] implemented in the CCP4 package.[72] For the R_{free} calculation, a randomly selected 10% of the reflections were used throughout the refinement process. Data processing and the structure refinement statistics are given in Table 1. There are no discernible differences among the structures obtained under conditions of low Mg/low Ca, 5 mM Mg^{2+}/10 mM Ca^{2+}, and 5 mM Mg^{2+}/20 mM Ca^{2+}. Consequently, only the low Mg/low Ca coordinates and structure factors are deposited in the RCSB Protein Data Bank (3TH2). The coordinates and structure factors for 2.5 mM Ca^{2+}/1.25 mM Mg^{2+} condition and for low Mg/high Ca condition are deposited into the Protein Data Bank with accession codes 3TH3 and 3TH4, respectively. The 1LQV coordinates[27] of APC-Gla/sEPCR complex were refined by replacing Ca^{2+} with Mg^{2+} at positions 1, 4 and 7 individually and/or in combination. The new coordinates and the structure factors are deposited with the accession code 3JTC.

Ca^{2+}-binding to dEGR-APC, decarboxylated dEGR-APC, WT-Protein C and D71K/E225K Protein C

Calcium binding was determined by equilibrium dialysis using $^{45}Ca^{2+}$ as described earlier.[12] The concentration of dEGR-APC, decarboxylated dEGR-APC, WT-Protein C or D71K/E225K Protein C used was 30 μM. The buffer used was TBS, pH 7.4.

D-FFR-VIIa and dEGR-APC binding to PC/PS phospholipid bilayer using SPR

Binding of D-FFR-VIIa and dEGR-APC to the PC/PS phospholipid bilayer in the presence and absence of Mg^{2+} was investigated using a Biacore T100 instrument. Liposomes (75% PC/25% PS), ~100 nm in diameter, were prepared by the extrusion method according to Erb *et al*.[73] A Biacore T100 L1 series chip and HBS, pH 7.4 buffer were used for all experiments. The sensor surface was charged with 20 mM Chaps at 20 μl/ml for 3 min, and this was followed by loading 1 mM PC/PS suspension at 3 μl/min for 17 min. The surface was washed (five cycles) with 30 mM EDTA/HBS, pH 7.4 at 20 μl/min for 3 min. The RU obtained were 4500 to 5600 between different couplings and the excess surface was blocked with bovine serum albumin (BSA). For a control surface, 1 mM PC was loaded onto the sensor surface in the same manner. For binding experiments, D-FFR-VIIa (0.5 μM–16 μM) or dEGR-APC (0.2 μM–3.2 μM) in HBS/BSA, pH 7.4 containing varying concentrations of Ca^{2+} and Mg^{2+} was passed over the phospholipid bilayer, and association and dissociation were monitored at a 30 μl/min for 3 min each. The lipid surface was regenerated using 30 mM EDTA/HBS, pH 7.4 for 2 min at 20 μl/min, and this was followed by a 2-min wash with HBS, pH 7.4. Affinity and kinetic parameters were determined after double subtraction of the non-specific binding from the control (PC) surface and a blank buffer cycle. In separate experiments, the effect of physiological Mg^{2+} on the phospholipid binding (as reflected in response units) was assessed using a constant concentration of D-FFR-VIIa or dEGR-APC and varying Ca^{2+} concentrations.

Activation of FX and ^{3}H-FIX by LPS stimulated human monocytes and microparticles

FVIIa (1 nM) in HBS/BSA, pH 7.4 containing varying concentrations of Ca^{2+} and Mg^{2+} was incubated with 12-hr LPS-stimulated monocytes (10^6 cells/ml) or microparticles (obtained from 10^6 cells and suspended in 1 ml) for 5 min at 37°C at which point FX or ^{3}H-FIX was added (100 nM, final concentration). Twenty μl aliquots were withdrawn at selected times (0–20 min), quenched with 25 mM EDTA, pH 8.0 and briefly centrifuged to remove cellular particles. The chromogenic substrate S-2222 was then added at 0.2 mM and the hydrolysis monitored by change in the absorbance at 405 nm using the Spectramax 190 from Molecular Devices (Sunnyvale, CA, USA). In the absence of FX, hydrolysis of S-2222 was not detected. FXa formed was calculated from a standard curve prepared by serial dilutions of purified human FXa obtained from Haematologic Technologies Inc. (Essex Junction, VT, USA). ^{3}H-FIX activation was measured as described previously.[59]

Inactivation of FVa by APC

Phospholipid vesicles for these experiments contained PE (60% PC/20% PS/20% PE) and were prepared by the method of Husten *et al*.[74] The total phospholipid concentration was determined by the analysis of organic phosphate.[75] Stock solution of human FVa used was

710 μg/ml in TBS, pH 7.4 containing 2 mM Ca^{2+}. FVa activity was determined by a standard one-stage clotting assay using FV deficient plasma. In this assay, 50 μl of thromboplastin reagent was incubated with 50 μl of FV deficient plasma for 3 min at 37 °C. A 50-μl volume of FVa (diluted in TBS/BSA, pH 7.4 containing 2 mM Ca^{2+} at 37 °C) and 50 μl of 35 mM Ca^{2+} at 37 °C were then added simultaneously. The clotting time was recorded using the ThromboScreen® 400c instrument. A standard curve was constructed using known concentrations of FVa. Each reaction contained 120 nM FVa, 10 μM phospholipid, 8 nM APC and varying concentrations of Ca^{2+}/Mg^{2+} in TBS/BSA, pH 7.4. Aliquots were removed at different times, diluted 50- to 300-fold and assayed for FVa activity.

Accession numbers

Structure factors and coordinates of the final model of the FVIIa/sTF complexes and PC-Gla/sEPCR were deposited in the PDB and their accession codes are the following: low Mg/low Ca, 3TH2; 1.25 mM Mg^{2+}/2.5 mM Ca^{2+}, 3TH3; low Mg/high Ca, 3TH4 and PC-Gla/sEPCR, 3JTC. These are listed in Table 1.

Supplementary Material

Refer to Web version on PubMed Central for supplementary material.

Acknowledgments

This work was supported in part, by National Institute of Health grants RO1HL36365 and R21HL89661.

The abbreviations used are

VKD	vitamin K-dependent
Gla	γ-carboxyglutamic acid
APC	activated Protein C
TF	Tissue factor
sTF	soluble TF
BSA	bovine serum albumin
WT	Wild-type
D-FFR-ck	D-Phe-Phe-Arg chloromethylketone
dEGR-ck	dansyl-Glu-Gly-Arg chloromethylketone
FVa	activated factor V
FVII	factor VII
FVIIa	factor VIIa
FIX	factor IX
FIXa	factor IXa

FIX-bp	FIX binding protein
FX	factor X
FXa	factor Xa
LPS	lipopolysaccharide
PC	phosphatidylcholine
PE	phosphatidylethonolamine
PS	phosphatidylserine
sEPCR	soluble endothelial Protein C receptor
SPR	surface plasmon resonance
RU	Response Units
S-2222	*N*-benzoyl-L-isoleucyl-L-glutamyl-glycyl-L-arginine-*p*-nitroaniline
TFPI	tissue factor pathway inhibitor
TBS	0.05 M Tris/0.15 M NaCl, pH 7.5
TBS/BSA	TBS containing 0.1 mg/ml BSA
HBS	pH 7.4, 10 mM Hepes/0.15 M NaCl, pH 7.4
HBS/BSA	HBS containing 0.1 mg/ml BSA
Ca	calcium
Mg	magnesium

References

1. Nelsestuen GL, Shah AM, Harvey SB. Vitamin K-dependent proteins. Vitam. Horm. 2000; 58:355–389. [PubMed: 10668405]
2. Davie EW. A brief historical review of the waterfall/cascade of blood coagulation. J. Biol. Chem. 2003; 278:50819–50832. [PubMed: 14570883]
3. Wildhagen KC, Lutgens E, Loubele ST, ten Cate H, Nicolaes GA. The structure-function relationship of activated protein C. Lessons from natural and engineered mutations. Thromb. Haemost. 2011; 106:1034–1045. [PubMed: 22072231]
4. Esmon CT. Protein C anticoagulant system—anti-inflammatory effects. Semin. Immunopathol. 2012; 34:127–132. [PubMed: 21822632]
5. Soriano-Garcia M, Padmanabhan K, de Vos AM, Tulinsky A. The Ca^{2+} ion and membrane binding structure of the Gla domain of Ca-prothrombin fragment 1. Biochemistry. 1992; 31:2554–2566. [PubMed: 1547238]
6. Freedman SJ, Furie BC, Furie B, Baleja JD. Structure of the metal-free gamma-carboxyglutamic acid-rich membrane binding region of factor IX by two-dimensional NMR spectroscopy. J. Biol. Chem. 1995; 270:7980–7987. [PubMed: 7713897]
7. Freedman SJ, Furie BC, Furie B, Baleja JD. Structure of the calcium ion-bound gamma-carboxyglutamic acid-rich domain of factor IX. Biochemistry. 1995; 34:12126–12137. [PubMed: 7547952]
8. Sunnerhagen M, Forsén S, Hoffrén AM, Drakenberg T, Teleman O, Stenflo J. Structure of the Ca(2+)-free Gla domain sheds light on membrane binding of blood coagulation proteins. Nat. Struct. Biol. 1995; 2:504–509. [PubMed: 7664114]

9. Prendergast FG, Mann KG. Differentiation of metal ion-induced transitions of prothrombin fragment 1. J. Biol. Chem. 1977; 252:840–850. [PubMed: 838700]
10. Persson E, Björk I, Stenflo J. Protein structural requirements for Ca2+ binding to the light chain of factor X. Studies using isolated intact fragments containing the gamma-carboxyglutamic acid region and/or the epidermal growth factor-like domains. J. Biol. Chem. 1991; 266:2444–2452. [PubMed: 1989996]
11. Castellino FJ. Human protein C and activated protein C components of the human anticoagulation system. Trends. Cardiovasc. Med. 1995; 5:55–62. [PubMed: 21232238]
12. Bajaj SP, Schmidt AE, Agah S, Bajaj MS, Padmanabhan K. High resolution structures of p-aminobenzamidine- and benzamidine-VIIa/soluble tissue factor: unpredicted conformation of the 192–193 peptide bond and mapping of Ca^{2+}, Mg^{2+}, Na^{+}, and Zn^{2+} sites in factor VIIa. J. Biol. Chem. 2006; 281:24873–24888. [PubMed: 16757484]
13. Agah S, Bajaj SP. Role of magnesium in factor XIa catalyzed activation of factor IX: calcium binding to factor IX under physiologic magnesium. J. Thromb. Haemost. 2009; 7:1426–1428. [PubMed: 19500239]
14. Wang S, McDonnell EH, Sedor FA, Toffaletti JG. pH effects on measurements of ionized calcium and ionized magnesium in blood. Arch. Pathol. Lab. Med. 2002; 126:947–950. [PubMed: 12171493]
15. Sekiya F, Yamashita T, Atoda H, Komiyama Y, Morita T. Regulation of the tertiary structure and function of coagulation factor IX by magnesium (II) ions. J. Biol. Chem. 1995; 270:14325–14331. [PubMed: 7782291]
16. Sekiya F, Yoshida M, Yamashita T, Morita T. Localization of the specific binding site for magnesium (II) ions in factor IX. FEBS Lett. 1996; 392:205–208. [PubMed: 8774845]
17. Shikamoto Y, Morita T, Fujimoto Z, Mizuno H. Crystal structure of Mg^{2+}- and Ca^{2+}-bound Gla domain of factor IX complexed with binding protein. J. Biol. Chem. 2003; 278:24090–24094. [PubMed: 12695512]
18. Messer AS, Velander WH, Bajaj SP. Contribution of magnesium in binding of factor IXa to the phospholipid surface: implications for vitamin K-dependent coagulation proteins. J. Thromb. Haemost. 2009; 7:2151–2153. [PubMed: 19817987]
19. Wang SX, Hur E, Sousa CA, Brinen L, Slivka EJ, Fletterick RJ. The extended interactions and Gla domain of blood coagulation factor Xa. Biochemistry. 2003; 42:7959–7966. [PubMed: 12834348]
20. Persson E, Ostergaard A. Mg(2+) binding to the Gla domain of factor X influences the interaction with tissue factor. J. Thromb. Haemost. 2007; 5:1977–1978. [PubMed: 17723139]
21. Ishikawa M, Kumashiro M, Yamazaki Y, Atoda H, Morita T. Anticoagulant mechanism of factor IX/factor X-binding protein isolated from the venom of Trimeresurus flavoviridis. J Biochem. 2009; 145:123–128. [PubMed: 18977769]
22. Banner DW, D'Arcy A, Chène C, Winkler FK, Guha A, Konigsberg WH, Nemerson Y, Kirchhofer D. The crystal structure of the complex of blood coagulation factor VIIa with soluble tissue factor. Nature. 1996; 380:41–46. [PubMed: 8598903]
23. Ruf W, Shobe J, Rao SM, Dickinson CD, Olson A, Edgington TS. Importance of factor VIIa Gla-domain residue Arg-36 for recognition of the macromolecular substrate factor X Gla-domain. Biochemistry. 1999; 38:1957–1966. [PubMed: 10026279]
24. Ruf W, Miles DJ, Rehemtulla A, Edgington TS. Tissue factor residues 157–167 are required for efficient proteolytic activation of factor X and factor VII. J. Biol. Chem. 1992; 267:22206–22210. [PubMed: 1429572]
25. Rao LV, Ruf W. Tissue factor residues Lys165 and Lys166 are essential for rapid formation of the quaternary complex of tissue factor. VIIa with Xa. tissue factor pathway inhibitor. Biochemistry. 1995; 34:10867–10871. [PubMed: 7662667]
26. Huang Q, Neuenschwander PF, Rezaie AR, Morrissey JH. Substrate recognition by tissue factor-factor VIIa. Evidence for interaction of residues Lys165 and Lys166 of tissue factor with the 4-carboxyglutamate-rich domain of factor X. J. Biol. Chem. 1996; 271:21752–21757. [PubMed: 8702971]

27. Oganesyan V, Oganesyan N, Terzyan S, Qu D, Dauter Z, Esmon NL, Esmon CT. The crystal structure of the endothelial protein C receptor and a bound phospholipid. J. Biol. Chem. 2002; 277:24851–24854. [PubMed: 12034704]
28. Parr RG, Pearson RG. Absolute Hardness: Companion parameter to absolute electronegativity. J. Am. Chem. Soc. 1983; 105:7512–7516.
29. de Courcy B, Pedersen LG, Parisel O, Gresh N, Silvi B, Pilmé J, Piquemal JP. Understanding selectivity of hard and soft metal cations within biological systems using the subvalence concept. I. Application to blood coagulation: direct cation-protein electronic effects vs. indirect interactions through water networks. J. Chem. Theory Comput. 2010; 6:1048–1063. [PubMed: 20419068]
30. Ohkubo YZ, Tajkhorshid E. Distinct structural and adhesive roles of Ca^{2+} in membrane binding of blood coagulation factors. Structure. 2008; 16:72–81. [PubMed: 18184585]
31. Shaw AW, Pureza VS, Sligar SG, Morrissey JH. The local phospholipid environment modulates the activation of blood clotting. J. Biol. Chem. 2007; 282:6556–6563. [PubMed: 17200119]
32. Lu Y, Nelsestuen GL. Dynamic features of prothrombin interaction with phospholipid vesicles of different size and composition: implications for protein--membrane contact. Biochemistry. 1996; 35:8193–8200. [PubMed: 8679573]
33. Nelsestuen GL, Ostrowski BG. Membrane association with multiple calcium ions: vitamin-K-dependent proteins, annexins and pentraxins. Curr. Opin. Struct. Biol. 1999; 9:433–437. [PubMed: 10449363]
34. Erb EM, Stenflo J, Drakenberg T. Interaction of bovine coagulation factor X and its glutamic-acid-containing fragments with phospholipid membranes. A surface plasmon resonance study. Eur. J. Biochem. 2002; 269:3041–3046. [PubMed: 12071969]
35. Huang M, Rigby AC, Morelli X, Grant MA, Huang G, Furie B, Seaton B, Furie BC. Structural basis of membrane binding by Gla domains of vitamin K-dependent proteins. Nat. Struct. Biol. 2003; 10:751–756. [PubMed: 12923575]
36. Morrissey JH, Tajkhorshid E, Rienstra CM. Nanoscale studies of protein-membrane interactions in blood clotting. J Thromb Haemost. 2011; 9(S1):162–167. [PubMed: 21781251]
37. The PyMOL Molecular Graphics System, Version 1.5.0.4. Schrödinger, LLC;
38. Bjelke JR, Olsen OH, Fodje M, Svensson LA, Bang S, Bolt G, Kragelund BB, Persson E. Mechanism of the Ca^{2+}-induced enhancement of the intrinsic factor VIIa activity. J. Biol. Chem. 2008; 283:25863–25870. [PubMed: 18640965]
39. Liaw PC, Neuenschwander PF, Smirnov MD, Esmon CT. Mechanisms by which soluble endothelial cell protein C receptor modulates protein C and activated protein C function. J. Biol. Chem. 2000; 275:5447–5452. [PubMed: 10681521]
40. Yang C, Pflugrath JW. Applications of anomalous scattering from S atoms for improved phasing of protein diffraction data collected at Cu Kα wavelength. Acta Cryst. D. 2001; 57:1480–1490. [PubMed: 11567163]
41. Colpitts TL, Castellino FJ. Calcium and phospholipid binding properties of synthetic gamma-carboxyglutamic acid-containing peptides with sequence counterparts in human protein C. Biochemistry. 1994; 33:3501–3508. [PubMed: 8142347]
42. Schmidt AE, Padmanabhan K, Underwood MC, Bode W, Mather T, Bajaj SP. Thermodynamic linkage between the S1 site, the Na^{+} site, and the Ca^{2+} site in the protease domain of human activated protein C (APC). Sodium ion in the APC crystal structure is coordinated to four carbonyl groups from two separate loops. J. Biol. Chem. 2002; 277:28987–28995. [PubMed: 12029084]
43. Smirnov MD, Esmon CT. Phosphatidylethanolamine incorporation into vesicles selectively enhances factor Va inactivation by activated protein C. J. Biol. Chem. 1994; 269:816–819. [PubMed: 8288632]
44. Nelsestuen GL. Enhancement of vitamin-K-dependent protein function by modification of the gamma-carboxyglutamic acid domain: studies of protein C and factor VII. Trends Cardiovasc. Med. 1999; 9:162–167. [PubMed: 10639722]
45. Ghosh S, Pendurthi UR, Steinoe A, Esmon CT, Rao LV. Endothelial cell protein C receptor acts as a cellular receptor for factor VIIa on endothelium. J. Biol. Chem. 2007; 282:11849–11857. [PubMed: 17327234]
46. Pearson RG. Chemical hardness and density functional theory. J. Chem. Sci. 2005; 117:369–377.

47. Jiao D, King C, Grossfield A, Darden TA, Ren P. Simulation of Ca^{2+} and Mg^{2+} solvation using polarizable atomic multipole potential. J. Phys. Chem. B. 2006; 110:18553–18559. [PubMed: 16970483]
48. Glusker JP, Katz AK, Bock CW. Metal ions in biological systems. Rigaku J. 1999; 16:8–17.
49. Shen L, Shah AM, Dahlbäck B, Nelsestuen GL. Enhancement of human protein C function by site-directed mutagenesis of the gamma-carboxyglutamic acid domain. J. Biol. Chem. 1998; 273:31086–31091. [PubMed: 9813008]
50. Harvey SB, Stone MD, Martinez MB, Nelsestuen GL. Mutagenesis of the gamma-carboxyglutamic acid domain of human factor VII to generate maximum enhancement of the membrane contact site. J. Biol. Chem. 2003; 278:8363–8369. [PubMed: 12506121]
51. Sekiya F, Yoshida M, Yamashita T, Morita T. Magnesium(II) is a crucial constituent of the blood coagulation cascade. Potentiation of coagulant activities of factor IX by Mg^{2+} ions. J. Biol. Chem. 1996; 271:8541–8544. [PubMed: 8621478]
52. Lee CJ, Chandrasekaran V, Wu S, Duke RE, Pedersen LG. Recent estimates of the structure of the factor VIIa (FVIIa)/tissue factor (TF) and factor Xa (FXa) ternary complex. Thromb. Res. 2010; 125:S7–S10. [PubMed: 20156644]
53. Bajaj MS, Ghosh M, Bajaj SP. Fibronectin-adherent monocytes express tissue factor and tissue factor pathway inhibitor whereas endotoxin-stimulated monocytes primarily express tissue factor: physiologic and pathologic implications. J. Thromb. Haemost. 2007; 5:1493–1499. [PubMed: 17470199]
54. Yam LT, Li CY, Crosby WH. Cytochemical identification of monocytes and granulocytes. Am. J. Clin. Pathol. 1971; 55:283–290. [PubMed: 5549896]
55. Tolnai S. A method for viable cell count. Methods Cell Sci. 1975; 1:37–38.
56. Abid Hussein MN, Meesters EW, Osmanovic N, Romijn FP, Nieuwland R, Sturk A. Antigenic characterization of endothelial cell-derived microparticles and their detection ex vivo. J. Thromb. Haemost. 2003; 1:2434–2443. [PubMed: 14629480]
57. Bajaj SP, Rapaport SI, Prodanos C. A simplified procedure for purification of human prothrombin, factor IX and factor X. Prep. Biochem. 1981; 11:397–412. [PubMed: 7312833]
58. Van Lenten L, Ashwell G. Studies on the chemical and enzymatic modification of glycoproteins. A general method for the tritiation of sialic acid-containing glycoproteins. J. Biol. Chem. 1971; 246:1889–1894. [PubMed: 4323238]
59. Bajaj SP, Birktoft JJ. Human factor IX and factor IXa. Methods Enzymol. 1993; 222:96–128. [PubMed: 8412817]
60. Buddai SK, Toulokhonova L, Bergum PW, Vlasuk GP, Krishnaswamy S. Nematode anticoagulant protein c2 reveals a site on factor Xa that is important for macromolecular substrate binding to human prothrombinase. J. Biol. Chem. 2002; 277:26689–26698. [PubMed: 12011050]
61. Mathur A, Bajaj SP. Protease and EGF1 domains of factor IXa play distinct roles in binding to factor VIIIa. Importance of helix 330 (helix 162 in chymotrypsin) of protease domain of factor IXa in its interaction with factor VIIIa. J. Biol. Chem. 1999; 274:18477–18486. [PubMed: 10373456]
62. Bajaj SP, Price PA, Russell WA. Decarboxylation of gamma-carboxyglutamic acid residues in human prothrombin. Stoichiometry of calcium binding to gamma-carboxyglutamic acid in prothrombin. J. Biol. Chem. 1982; 257:3726–3731. [PubMed: 7061506]
63. Ndonwi M, Broze GJ Jr, Agah S, Schmidt AE, Bajaj SP. Substitution of the Gla domain in factor X with that of protein C impairs its interaction with factor VIIa/tissue factor: lack of comparable effect by similar substitution in factor IX. J. Biol. Chem. 2007; 282:15632–15644. [PubMed: 17387172]
64. Foster DC, Yoshitake S, Davie EW. The nucleotide sequence of the gene for human protein C. Proc. Natl. Acad. Sci. USA. 1985; 82:4673–4677. [PubMed: 2991887]
65. Geng JP, Cheng CH, Castellino FJ. Functional consequences of mutations in amino acid residues that stabilize calcium binding to the first epidermal growth factor homology domain of human protein C. Thromb. Haemost. 1996; 76:720–728. [PubMed: 8950780]
66. Bode W, Mayr I, Baumann U, Huber R, Stone SR, Hofsteenge J. The refined 1.9Å crystal structure of human alpha-thrombin: interaction with D-Phe-Pro-Arg chloromethylketone and significance of the Tyr-Pro-Pro-Trp insertion segment. EMBO J. 1989; 8:3467–3475. [PubMed: 2583108]

67. Laemmli UK. Cleavage of structural proteins during the assembly of the head of bacteriophage T4. Nature. 1970; 227:680–685. [PubMed: 5432063]
68. Otwinowski Z, Minor W. Processing of X-ray diffraction data collected in oscillation mode. Methods Enzymol. 1997; 276:307–326.
69. Navaza J. AMoRe: an automated package for molecular replacement. Acta Cryst. 1994; A50:157–163.
70. Emsley P, Lohkamp B, Scott WG, Cowtan K. Features and development of Coot. Acta Cryst. 2010; D66:486–501.
71. Murshudov GN, Skubák P, Lebedev AA, Pannu NS, Steiner RA, Nicholls RA, Winn MD, Long F, Vagin AA. REFMAC5 for the refinement of macromolecular crystal structures. Acta Cryst. 2011; D67:355–367.
72. Collaborative Computational Project, 4. The CCP4 suite: programs for protein crystallography. Acta Cryst. 1994; D50:760–763.
73. Erb EM, Chen X, Allen S, Roberts CJ, Tendler SJ, Davies MC, Forsén S. Characterization of the surfaces generated by liposome binding to the modified dextran matrix of a surface plasmon resonance sensor chip. Anal. Biochem. 2000; 280:29–35. [PubMed: 10805517]
74. Husten EJ, Esmon CT, Johnson AE. The active site of blood coagulation factor Xa. Its distance from the phospholipid surface and its conformational sensitivity to components of the prothrombinase complex. J. Biol. Chem. 1987; 262:12953–12961. [PubMed: 3477541]
75. Lowry OH, Lopez JA. The determination of inorganic phosphate in the presence of labile phosphate esters. J. Biol. Chem. 1946; 162:421–428. [PubMed: 21018750]

- Plasma Ca^{2+} is insufficient to fold Gla domains in vitamin K-dependent proteins.
- Ca^{2+} and Mg^{2+} occupy specific sites in the Gla domains of factor VIIa and protein C.
- High Ca^{2+} or ligand binding to the ω-loop of Gla replaces Mg^{2+} at site 4 by Ca^{2+}
- Ca^{2+}occupancy at site 4 results in the active conformation of the ω-loop.
- Physiological Ca^{2+}/Mg^{2+} act in concert to promote coagulation and anticoagulation.

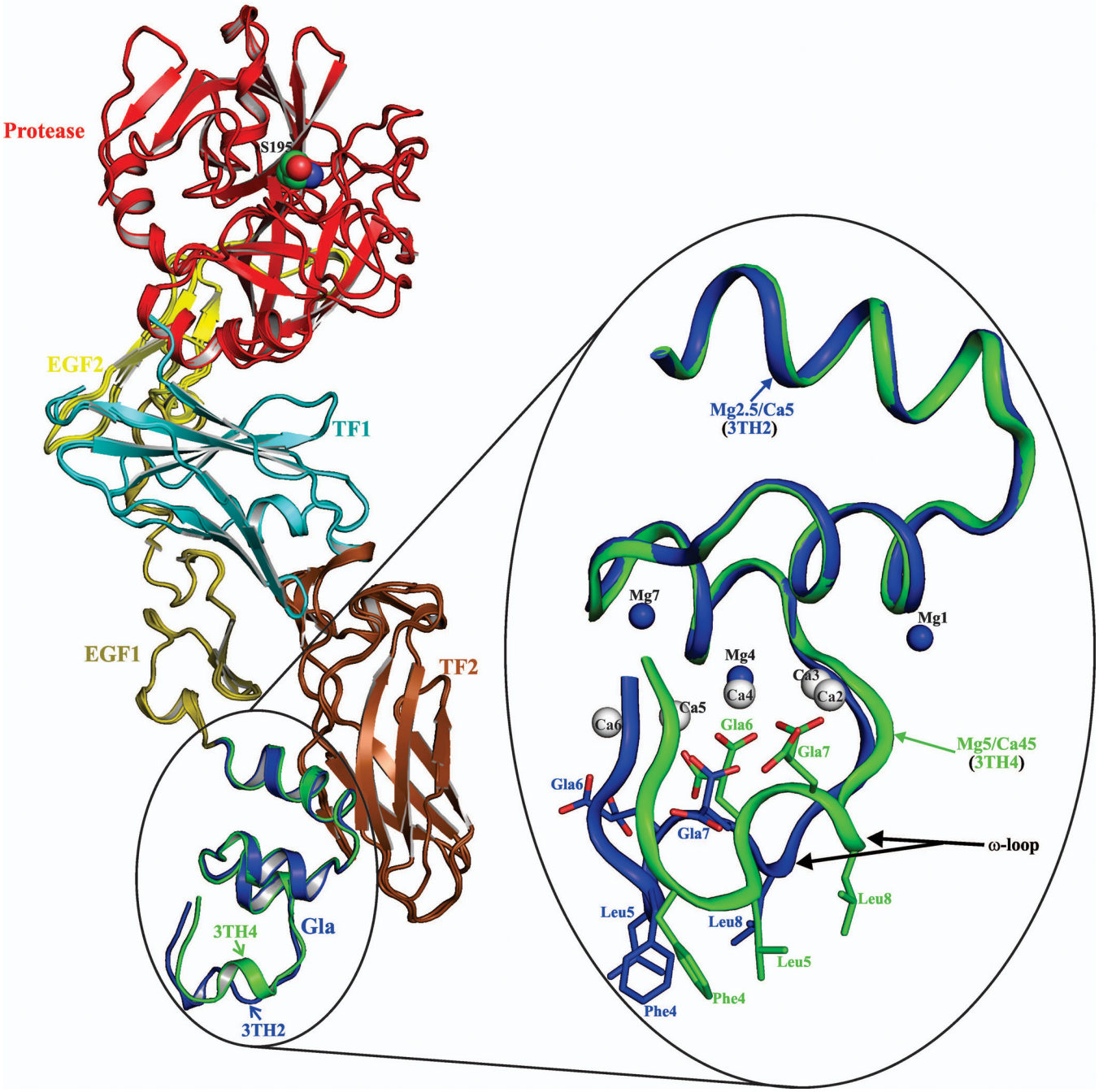

Figure 1. The structure of the FVIIa/sTF complex in the presence of Ca^{2+}/Mg^{2+}

The cartoon representations of the FVIIa/sTF complexes are shown on the left. In FVIIa, the Gla domain is in blue for 3TH2 (low Mg/low Ca) and in green for 3TH4 (low Mg/high Ca), EGF1 is in olive, EGF2 is in yellow and the protease domain is in red. In sTF, TF1 and TF2 domains are colored cyan and brown, respectively. The Gla domains of FVIIa with locations of the Ca^{2+} and Mg^{2+} sites under two different concentrations of Ca^{2+}/Mg^{2+} are shown in the expanded view on the right. Low Mg/low Ca condition (2.5 mM Mg^{2+}/5 mM Ca^{2+}), blue (3TH2); low Mg/high Ca condition (5 mM Mg^{2+}/45 mM Ca^{2+}), green (3TH4). Note the

distinct conformations of the ω-loop when position 4 is occupied by Mg^{2+} or Ca^{2+}. The structures were superimposed using Pymol.[37] The metal sites are numbered according to Tulinsky and coworkers.[5] Ca^{2+} and Mg^{2+} are shown as white and blue spheres, respectively. The Gla residues and the hydrophobic residues Phe4, Leu5, and Leu8 in the ω-loop involved in phospholipid binding are shown in stick representation. Ca, calcium; Mg, magnesium.

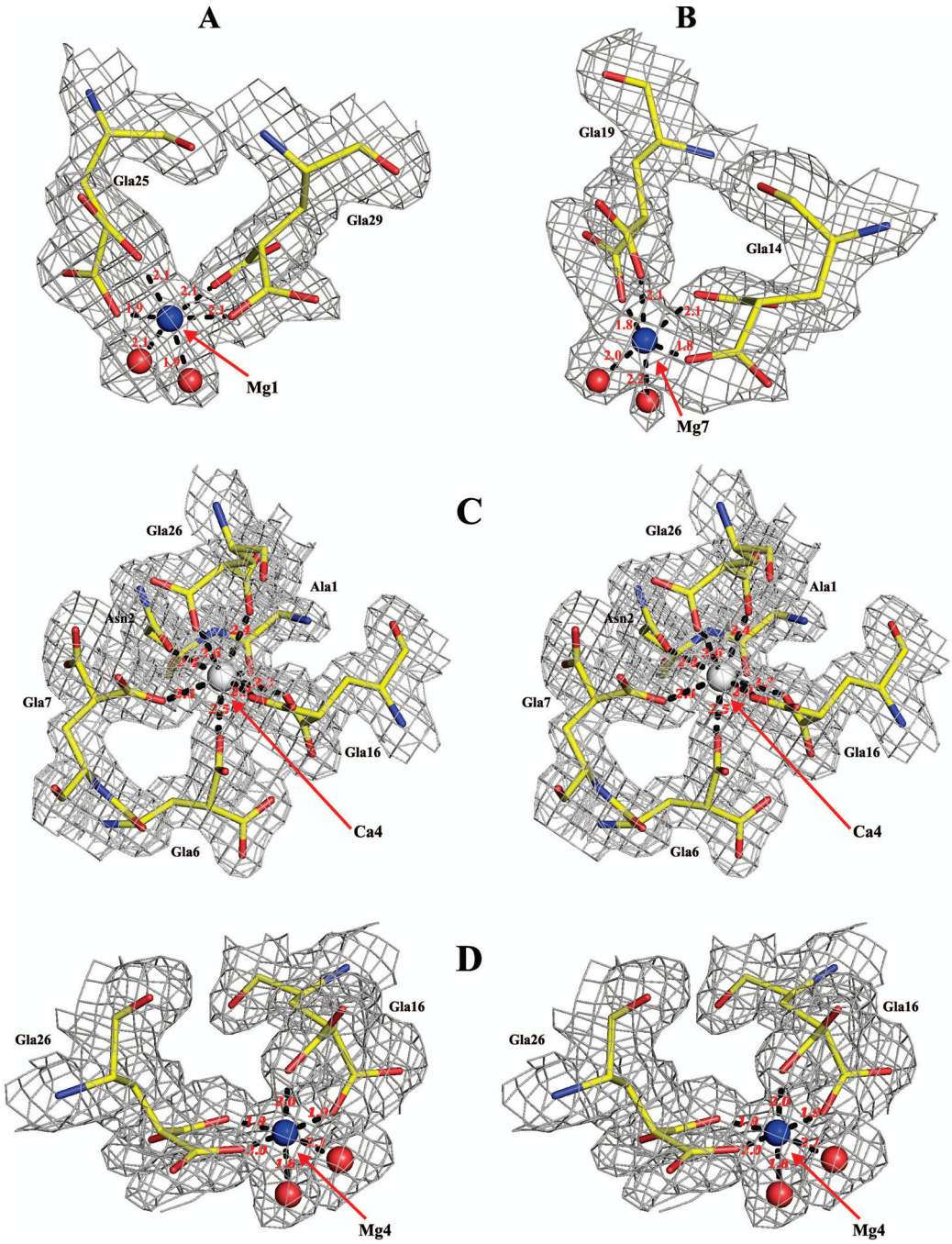

Figure 2. Coordination geometries of Mg^{2+} and Ca^{2+} in the FVIIa-Gla domain at positions 1, 4 and 7

Coordination of Mg^{2+} each at positions 1 and 7 (*panel A* and *panel B*), and of Ca^{2+} at position 4 (*panel C*) in the 3TH4 structure (low Mg/high Ca condition), along with the coordination of Mg^{2+} at position 4 (*panel D*) in the 3TH2 structure (low Mg/low Ca condition) are shown. Note that representations in panel C and panel D are in stereo. The electron density maps ($2F_{obs}$-F_{calc}) contoured at 1.0 σ are in gray. The coordination distances are in Angstroms depicted as black dashed lines. Ca^{2+}, Mg^{2+} and water molecules

are shown as white, blue and red spheres, respectively. Carbon, yellow; nitrogen, blue; and oxygen, red. Note that as compared to Mg4, water molecules do not serve as ligands for Ca4.

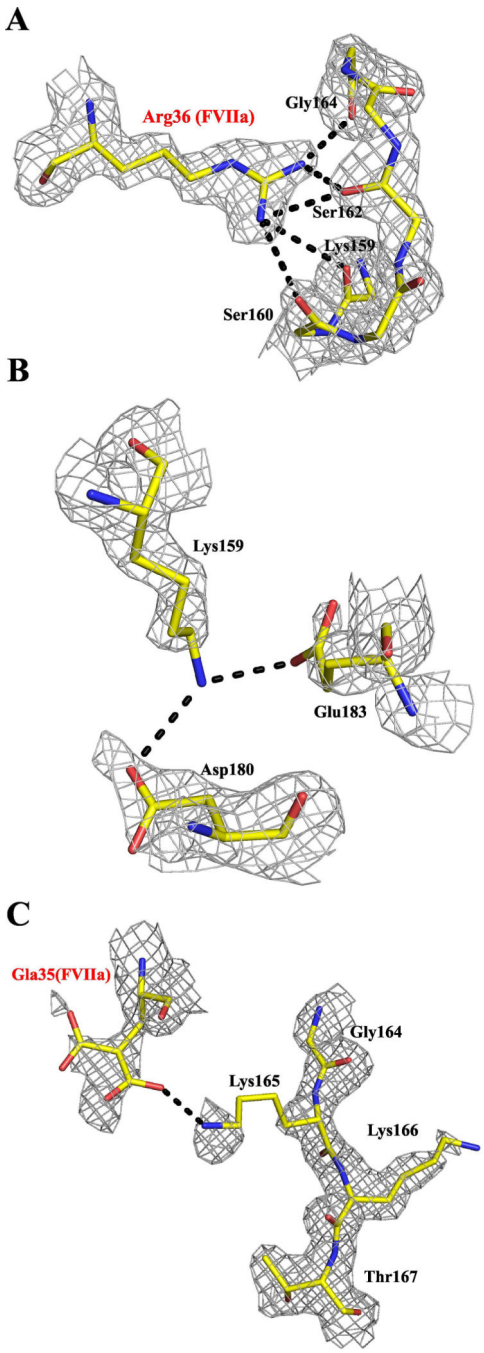

Figure 3. The 159–166 loop residues in sTF and their interactions with neighboring residues in the low Mg/low Ca structure

A, Residue Arg36 of FVIIa makes a network of hydrogen bonds with sTF residues in the 159–165 loop. *B*, Residue Lys159 of sTF makes bifurcated hydrogen bonds with Asp180 and Glu183 of sTF. *C*, Residue Lys165 of sTF makes a salt bridge with Gla35 of FVIIa. The electron density maps ($2F_{obs}$-F_{calc}) are contoured at 1.0 σ. Residues are shown in stick representation and hydrogen bonds in black dashed lines. As in Fig. 2, carbons are yellow, nitrogens are blue and oxygens are red.

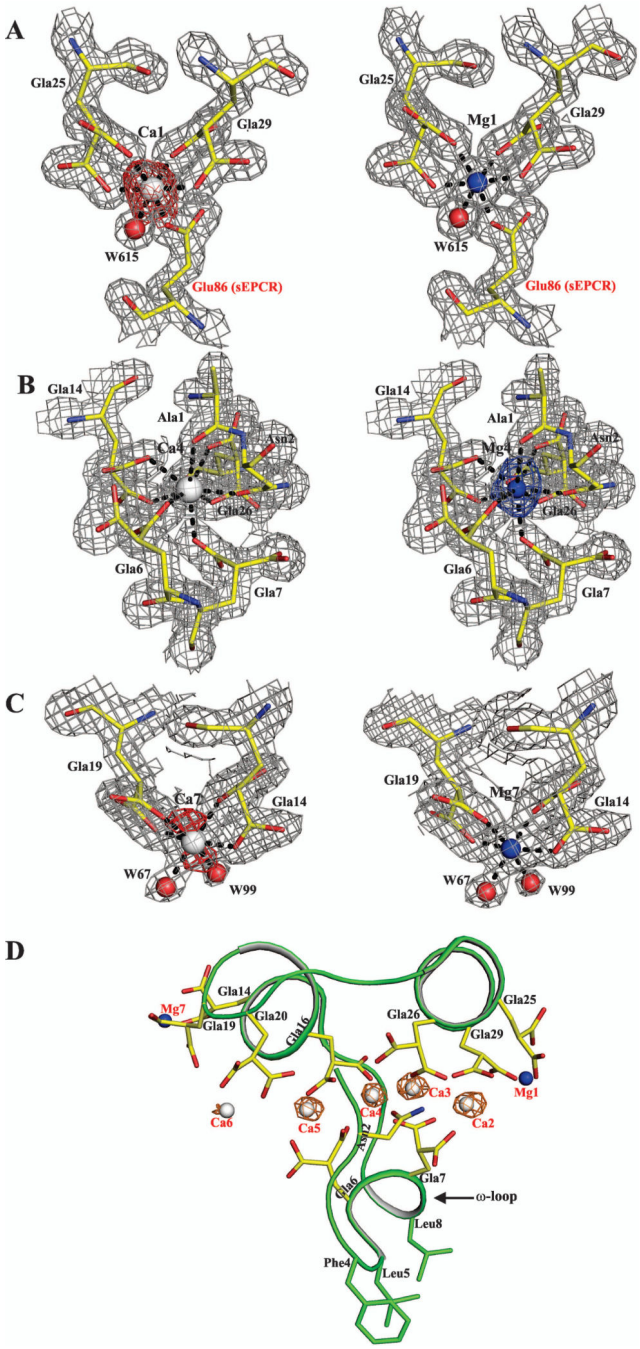

Figure 4. Metal specificity at sites 1, 4 and 7 in the APC-Gla/sEPCR structure under low Mg/low Ca condition

Metal sites at positions 1, 4 and 7 refined with Ca^{2+} are shown on the left in panels *A*, *B* and *C*. Metal sites at positions 1, 4 and 7 refined with Mg^{2+} are shown on the right in panels *A*, *B* and *C*. The electron density ($2F_{obs} - F_{calc}$) maps are contoured at 1 σ and the difference ($F_{obs} - F_{calc}$) maps are contoured at 2.5 σ. In the difference maps, the negative densities are shown in red and the positive density in blue. Panel *D* shows a cartoon representation of the APC-Gla domain with the anomalous map for (in orange) Ca^{2+} contoured at 3σ. In all

panels, the residues are shown in stick representation. The Ca^{2+}, Mg^{2+} and water (w) molecules are shown as white, blue and red spheres, respectively.

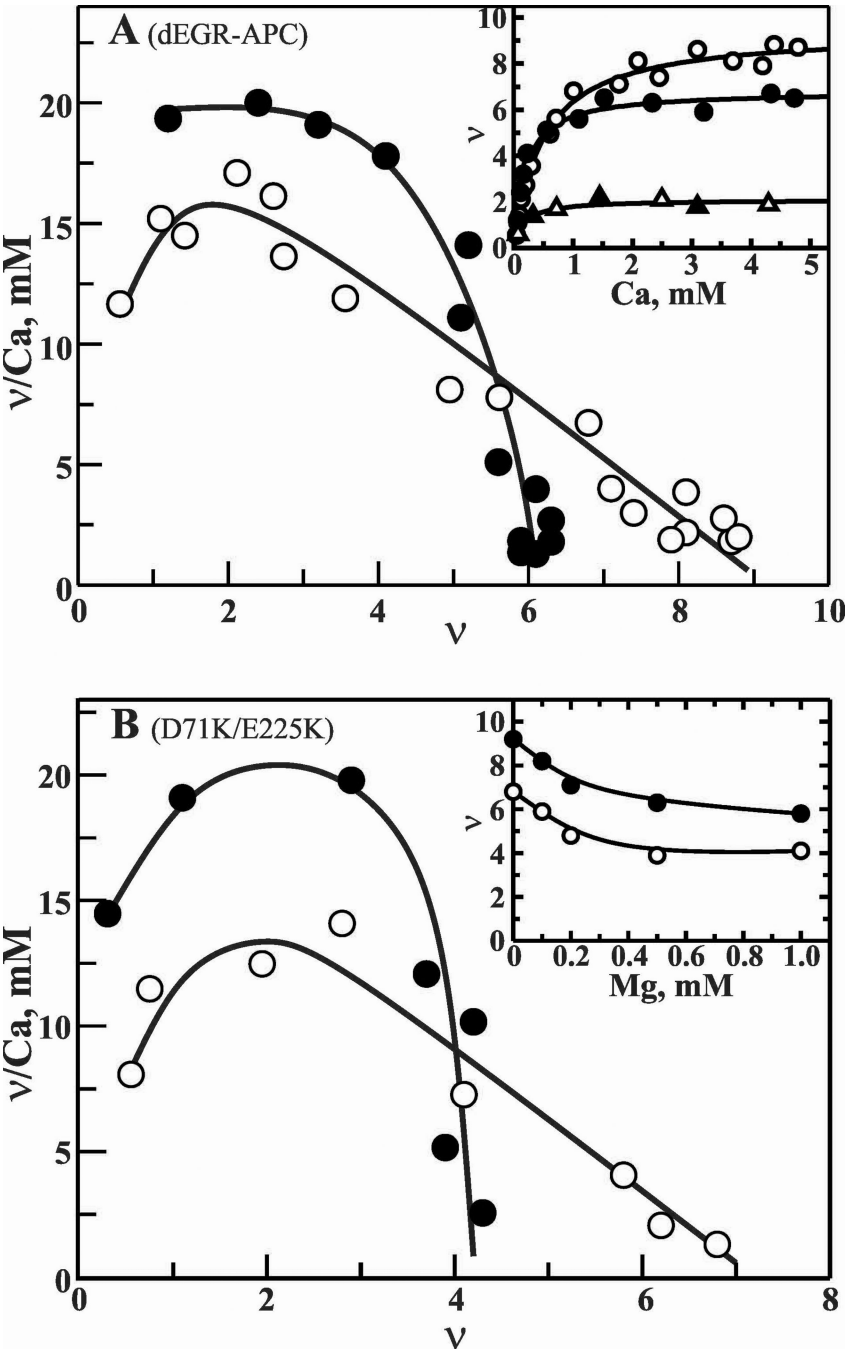

Figure 5. Scatchard plots of Ca^{2+}-binding to dEGR-APC, decarboxylated dEGR-APC and D71K/E225K Protein C

A, Ca^{2+} binding to APC. The moles of Ca^{2+} bound/mol of dEGR-APC (ν) are plotted against ν/Ca^{2+}, where Ca^{2+} is the free ligand concentration. Ca^{2+}-binding was measured by the technique of equilibrium dialysis using $^{45}Ca^{2+}$ as described under ″Materials and Methods″. A solution of 30 μM dEGR-APC was titrated with a series of Ca^{2+} solutions (0.1 to 5 mM) in the absence (○) presence of 0.6 mM Mg^{2+} (●). *Inset*, Direct plots of binding of Ca^{2+} to dEGR-APC/zero mM Mg^{2+} (○), dEGR-APC/0.6 mM Mg^{2+} (●), decarboxylated dEGR-APC/zero mM Mg^{2+} (△), and decarboxylated dEGR-APC/0.6 mM Mg^{2+}(▲). *B*,

Ca^{2+} binding to D71K/E225K Protein C. Data are plotted as in *A*. Ca^{2+} binding in the absence (○) or presence of 0.6 mM Mg^{2+} (●). *Inset*, displacement of Ca^{2+} by Mg^{2+}. Ca^{2+} sites were determined in the presence of various concentrations of Mg^{2+} at 3 mM constant Ca^{2+}. WT-Protein C (●) and E71K/E225K Protein C (○).

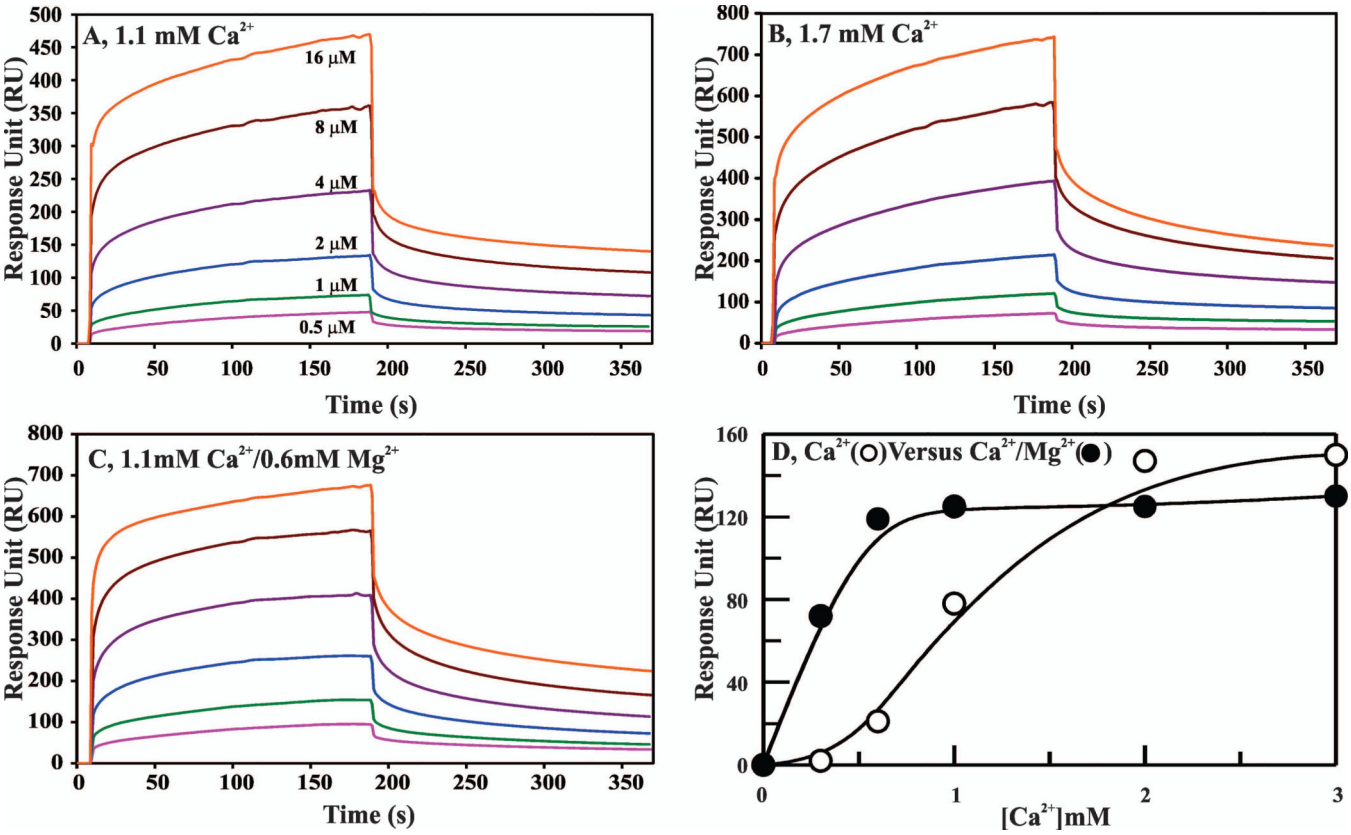

Figure 6. Contribution of Mg^{2+} to the binding of D-FFR-VIIa to PC/PS phospholipid bilayer as measured by SPR

A Biacore T100 L1 series chip and 10 mM Hepes/0.15 M NaCl, pH 7.4 (HBS, pH 7.4) were used for all experiments. The sample flow cell surface was charged with Liposomes (75% PC/25% PS) as described in ″Materials and Methods″. For a control surface, PC was loaded onto the sensor surface in the same manner. For binding experiments, different concentrations of D-FFR-VIIa were passed over the phopholipid bilayer, and association and dissociation were monitored at 30 μl min^{-1} for 3 min each. *A*, D-FFR-VIIa binding to phospholipid in 1.1 mM Ca^{2+}. The D-FFR-FVIIa concentrations used were: 0.5 μM (pink), 1 μM (green), 2 μM (blue), 4 μM (purple), 8 μM (brown), and 16 μM (red). *B*, D-FFR-VIIa binding to phospholipid in 1.7 mM Ca^{2+}. The D-FFR-FVIIa concentrations were the same as in ′*panel A*′. *C*, D-FFR-VIIa binding to phospholipid in 1.1 mM Ca^{2+}/0.6 mM Mg^{2+}. The D-FFR-VIIa concentrations were the same as in ′*panel A*′. Note that the Y-scale is different in ′*panel A*′ as compared to the ′*panels B* and *C*′. *D*, Effect of Mg^{2+} on the Ca^{2+} dependence of D-FFR-FVIIa binding to phospolipid. D-FFR-FVIIa (800 nM) binding (proportional to RUs) to the PC/PS bilayer was measured at varying concentrations of Ca^{2+} in the absence (○) or the presence (●) of 0.6 mM Mg^{2+}.

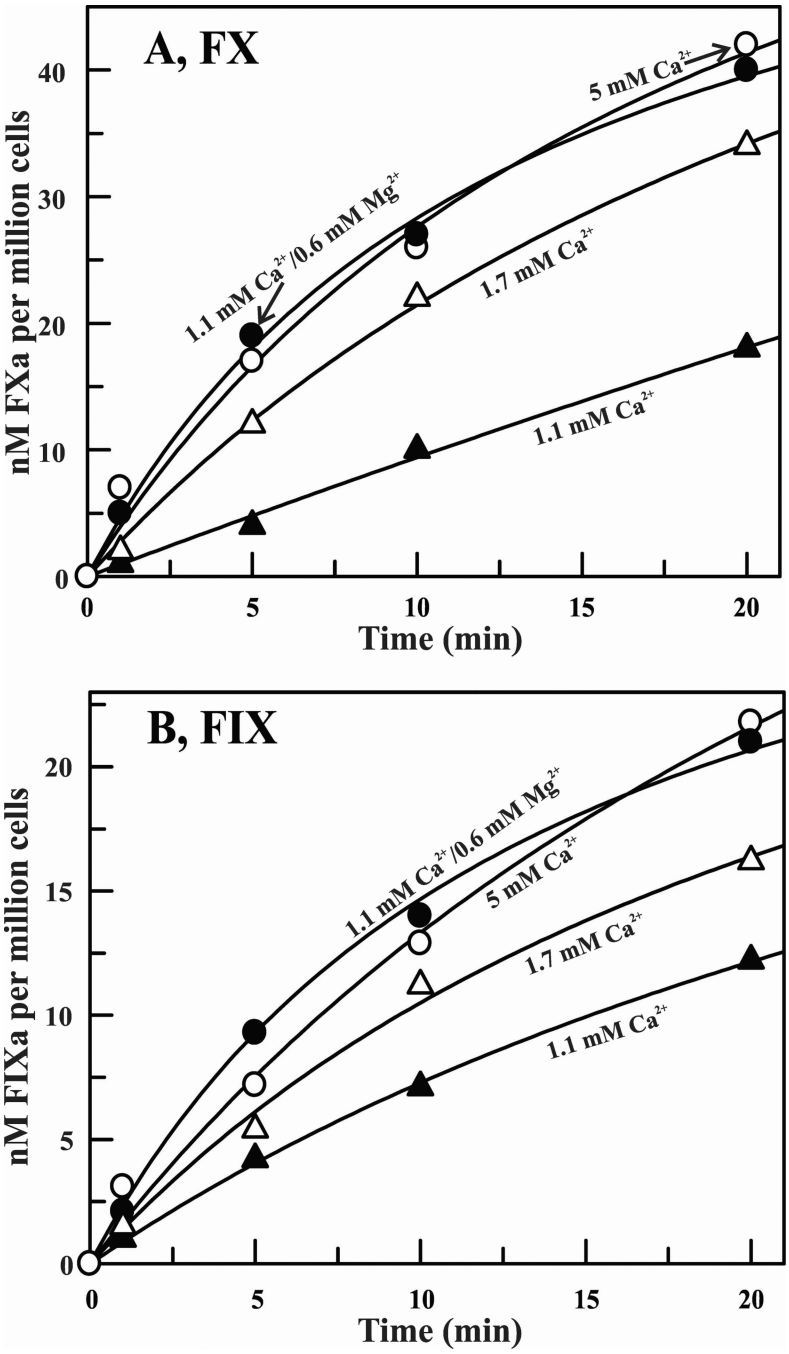

Figure 7. Effect of Mg^{2+} on the activations of FX and ^{3}H-FIX by FVIIa/TF assembled on LPS stimulated human monocytes

A, Activation of FX by FVIIa in the presence of 10^6 cells/ml. Concentration of FX was 100 nM and of FVIIa was 1 nM. FXa formation was monitored as described under ″Materials and Methods″. *B*, Activation of ^{3}H-FIX by FVIIa in the presence of 10^6 cells/ml. Concentration of ^{3}H-FIX was 100 nM and of FVIIa was 1 nM. ^{3}H-FIXa formation was monitored as described under ″Materials and Methods″. In both ′*panel A*′ and ′*panel B*′, concentrations of Ca^{2+} and/or Mg^{2+} were: 1.1 mM Ca^{2+} (closed triangles); 1.7 mM Ca^{2+}

(open triangles); 1.1 mM Ca^{2+}/0.6 mM Mg^{2+} (closed circles); and 5 mM Ca^{2+} (open circles).

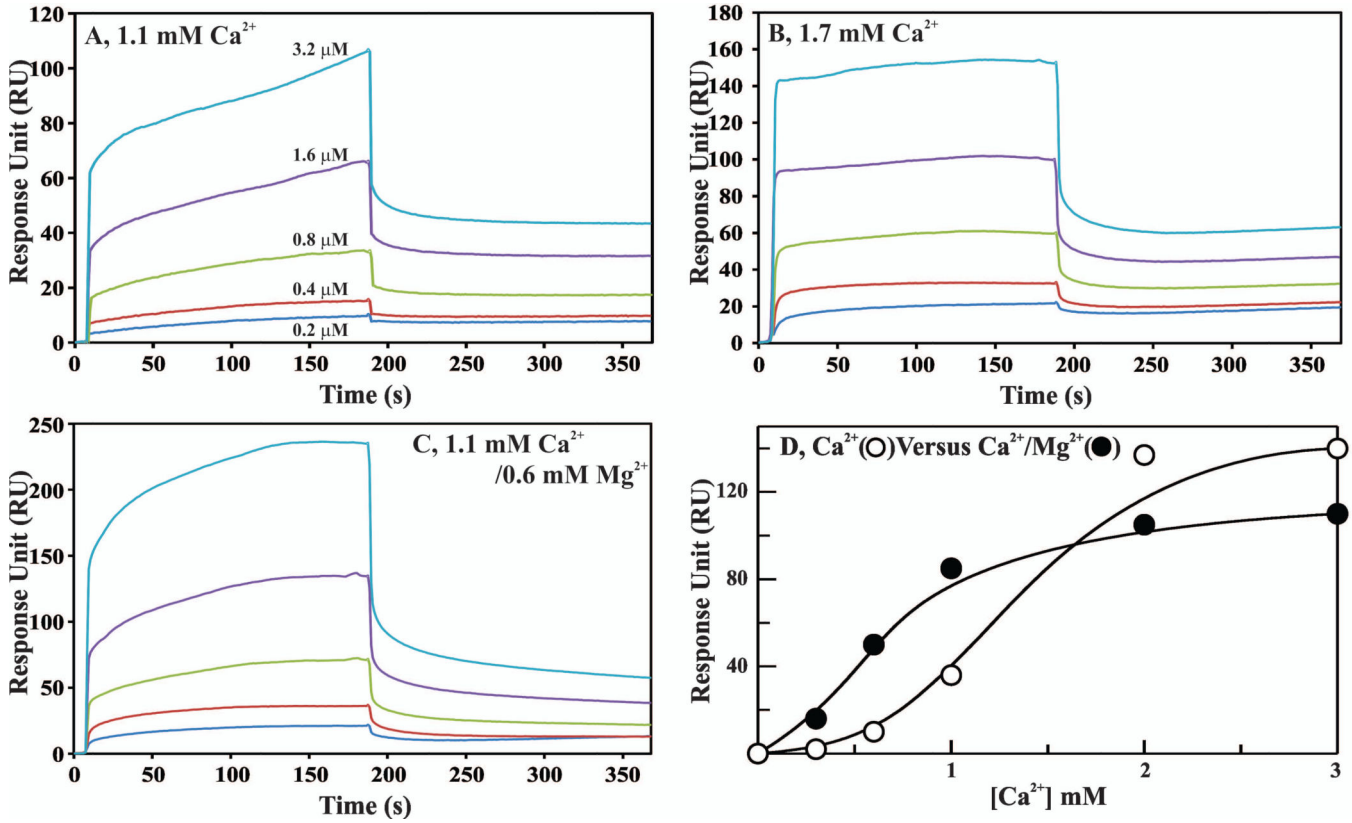

Figure 8. Contribution of Mg^{2+} to binding of dEGR-APC to the PC/PS phospholipid bilayer as measured by SPR

A Biacore T100 L1 series chip and HBS, pH 7.4 were used for all experiments. The sample flow cell surface was charged with Liposomes (75% PC/25% PS) as described in ″Materials and Methods″. For a control surface, PC was loaded onto the sensor surface in the same manner. For binding experiments, different concentrations of dEGR-APC were passed over the phospholipid bilayer, and association and dissociation were monitored at 30 μl min^{-1} for 3 min each. *A*, dEGR-APC binding to phopholipid in 1.1 mM Ca^{2+}. The dEGR-APC concentrations used were: 0.2 μM (blue), 0.4 μM (red), 0.8 μM (green), 1.6 μM (purple) and 3.2 μM (turquoise). *B*, dEGR-APC binding to phospholipid in 1.7 mM Ca^{2+}. The dEGR-APC concentrations were the same as in ′*panel A*′. *C*, dEGR-APC binding to phospholipid in 1.1 mM Ca^{2+}/0.6 mM Mg^{2+}. The dEGR-APC concentrations were the same as in ′*panel A*′. Note that the Y-scales are different between the ′*panel A, panel B and panel C*′. *D*, Effect of Mg^{2+} on the Ca^{2+} dependence of dEGR-APC binding to phopholipid. dEGR-APC (800 nM) binding (proportional to RUs) to PC/PS bilayer was measured at varying concentrations of Ca^{2+} in the absence (○) or the presence (●) of 0.6 mM Mg^{2+}.

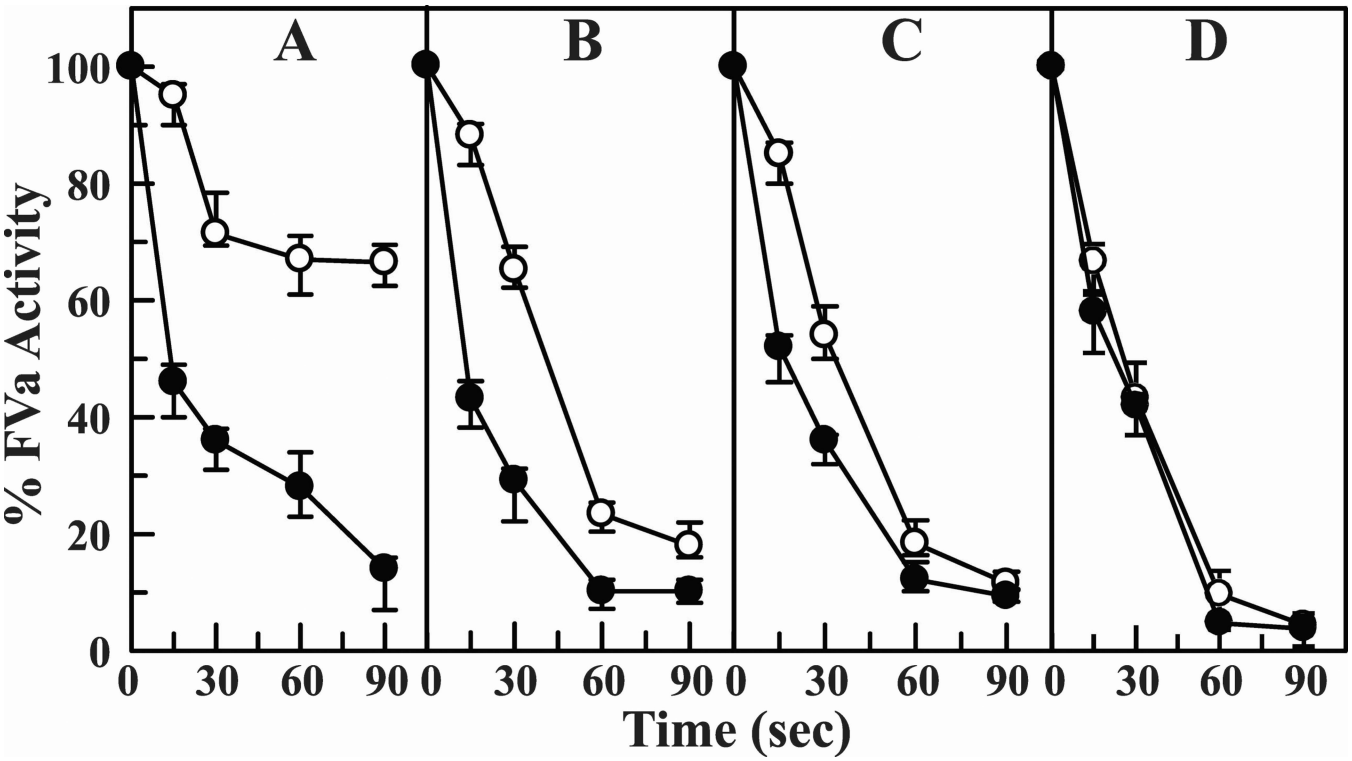

Figure 9. Effect of Mg^{2+} on the kinetics of inactivation of FVa by APC

Percent FVa residual activity is plotted against time. Inactivation was monitored by the decrease in FVa clotting activity as described in ″Materials and Methods″. APC was 8 nM, FVa was 120 nM and phospholipid was 10 μM. The reaction was carried out at 37 °C in buffer containing various concentrations Ca^{2+} (panel A, 0.5 mM Ca^{2+}; panel B, 0.8 mM Ca^{2+}; panel C, 1.1 mM Ca^{2+}; and panel D, 2 mM Ca^{2+}) in the absence (○) or presence of 0.6 mM Mg^{2+} (●). The results presented are the average of three experiments.

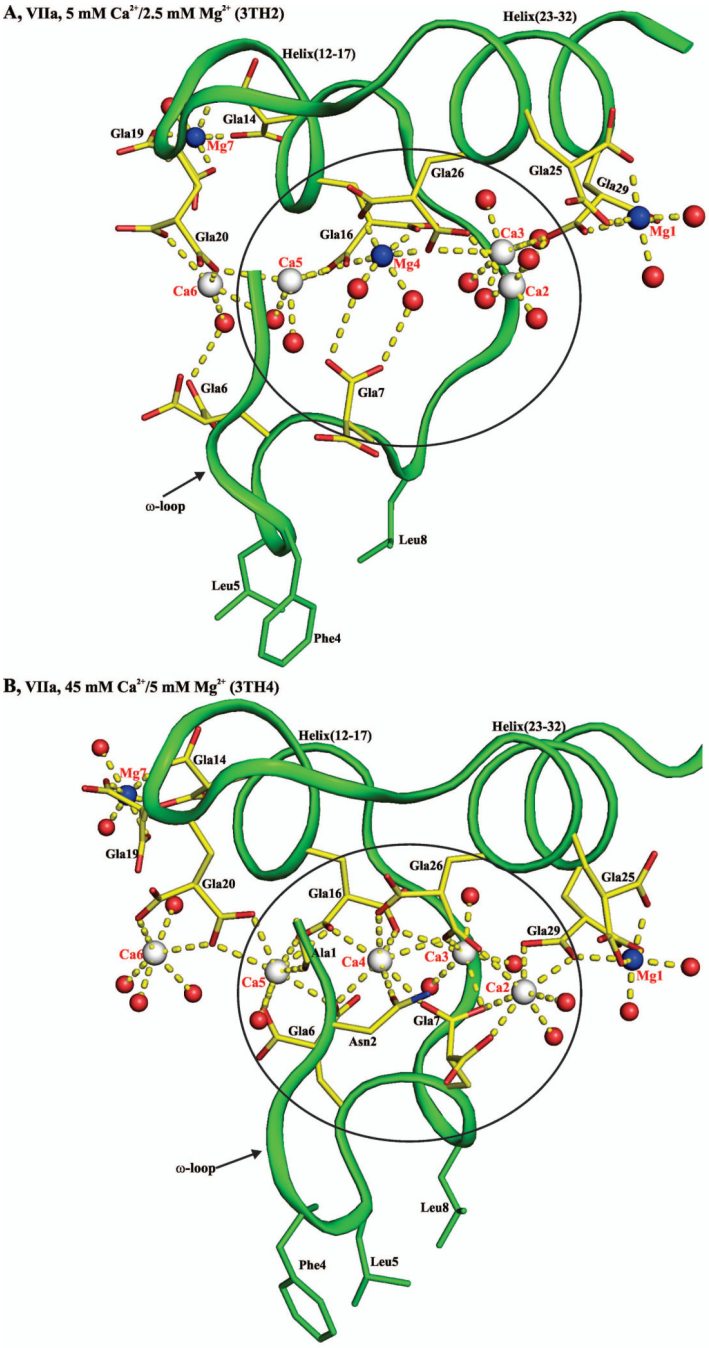

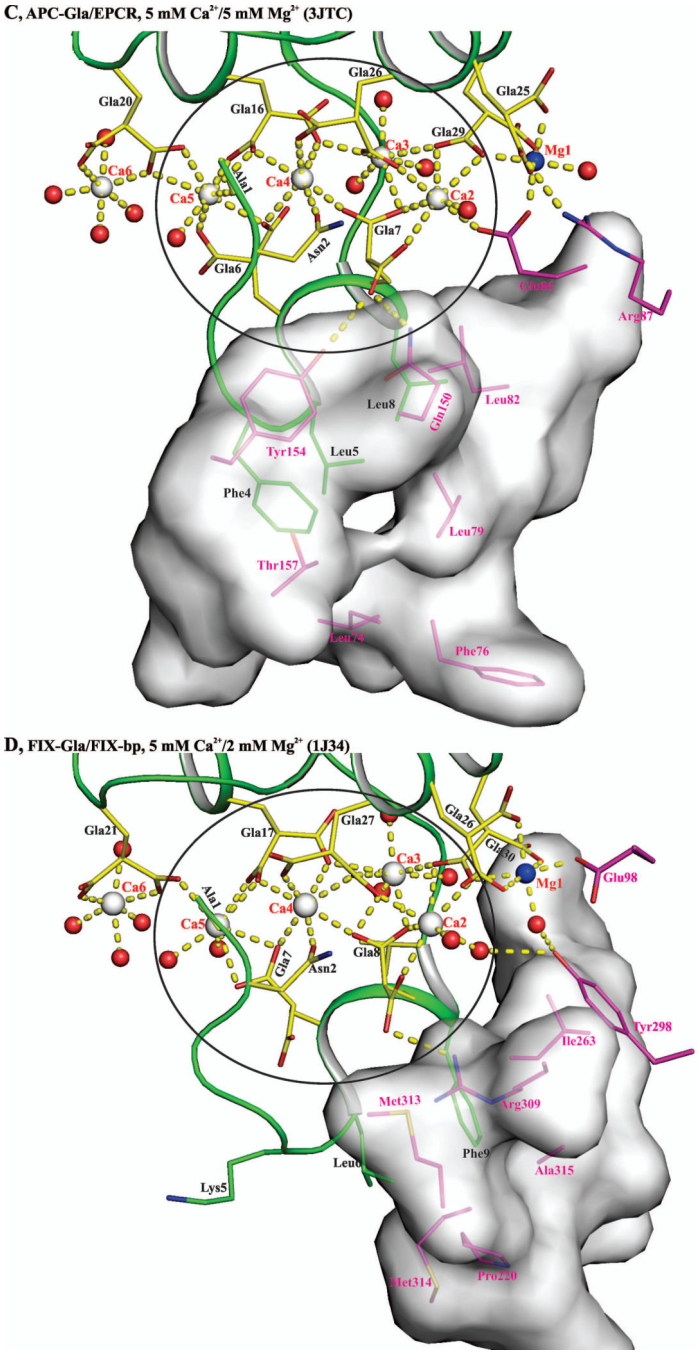

Figure 10. Contributing factors for occupancy of metal position 4 by Mg^{2+} or Ca^{2+} in the Gla domains of VKD proteins

A) Metal ion coordination in the FVIIa-Gla domain under low Mg/low Ca condition. Ca^{2+} and Mg^{2+} ions are bound in a linear fashion at the interface between the ω-loop and the two anti-parallel helices. The metal positions 1, 4 and 7 are occupied by Mg^{2+} and the other four sites are occupied by Ca^{2+}. The metal ions Ca2, Ca3, Mg4, and C5 coordinated to the Gla residues and to the ten water molecules are circled. *B*) Metal ion coordination in the FVIIa-Gla domain under the low Mg/high Ca. As in ′*panel A*′, the Ca^{2+} and Mg^{2+} ions are bound

at the interface between the helical segments and the ω-loop. The metal positions 1, and 7 are occupied by Mg^{2+} and the other five sites are occupied by Ca^{2+}. The metal ions Ca2, Ca3, Ca4, and Ca5 coordinated to the Gla residues and the six water molecules are circled. *C*) Metal ion coordination in the APC-Gla domain under low Mg/low Ca condition and its interaction with sEPCR. The sEPCR residues involved in hydrophobic interactions with APC-Gla domain are shown in stick representation. In sEPCR, only the region within 6 Å from the APC-Gla domain hydrophobic residues is shown in surface representation. The metal positions 1 and 7 are occupied by Mg^{2+} and the other five sites are occupied by Ca^{2+} as in ′*panel B*′ for the FVIIa-Gla domain. For clarity, Mg^{2+} site 7 is not shown. *D*) Metal ion coordination in the FIX-Gla domain under low Mg/low Ca condition and its interaction with FIX-bp. The FIX-bp residues involved in hydrophobic interactions with FIX-Gla domain are shown in stick representation. In FIX-bp, only the region within 6 Å from the FIX-Gla domain hydrophobic residues is shown in surface representation. The metal positions 1, 7 and 8 (unique to FIX) are occupied by Mg^{2+} and the other five sites are occupied by Ca^{2+}. Again for clarity, Mg^{2+} sites 7 and 8 are not shown. The sEPCR and FIX-bp residues are in magenta, whereas the Gla residues are in yellow. The hydrophobic residues present in the ω-loop are in green. The Ca^{2+}, Mg^{2+} and water molecule are depicted as white, blue and red spheres, respectively. The coordination contacts and the hydrogen bonds are shown in yellow dashed lines.

Table 1

Data Collection and Refinement statistics. Values in parentheses are for the highest resolution shell.

	dEGR-VIIa/sTF	Benzamidine-VIIa/sTF	dEGR-VIIa/sTF	APC-Gla/sEPCR
Crystal Condition	Mg5/Ca45[a]	Mg2.5/Ca5	Mg1.25/Ca2.5	Mg5/Ca5
PDB code	3TH4	3TH2	3TH3	3JTC
Space Group	$P2_12_12_1$	$P2_12_12_1$	$P2_1$	$P2_1$
Unit cell parameters (Å)				
A	69.91	69.94	78.07	59.22
B	81.23	80.87	68.89	62.36
C	126.53	126.43	79.15	71.03
α, β, γ (°)	90.0, 90.0, 90.0	90.0, 90.0, 90.0	90.0, 90.0, 90.0	90.0, 101.81, 90.0
Data Collection				
Beam Line	ALS	ALS	ALS	RIGAKURU300
Wave length (Å)	1.0	1.0	1.0	1.54
Resolution (Å)	68.36-1.8	61.20-1.72	78.08-2.70	30.0-1.55
Molecules per asymmetric unit	1	1	1	1
Measured reflections	291539	274959	79019	675700
Unique Reflections	65692	73836	22941	66375
Completeness (%)	97.7(99.6)	96.3(99.8)	98.8(93.1)	98.0(83.8)
Redundancy	4.4	3.7	3.4	10
$^{b}R_{merge}$	7.2(41.8)	6.6(50.0)	12.5(42.7)	5.0(45.5)
Average I/σ(I)	16.77(3.0)	18.28(3.05)	9.98(2.04)	34.0(4.03)
Refined Statistics				
Resolution (Å)	1.8	1.72	2.70	1.60
No. of atoms/residues				
Protein	4662	4707	3934	3422
Metal	75	42	65	198
Water	383	599	83	429
$^{c}R_{factor}$ (%)	20.4	18.4	22.8	19.1
$^{c}R_{free‡}$ (%)	23.4	22.9	29.8	22.6
r.m.s deviations from ideal values				
Bond Lengths (Å)	0.025	0.026	0.016	0.012
Bond Angles (°)	2.00	2.130	1.850	1.381
Ramachandran plot (%)				
Most favored regions (%)	89.5	90.7	84.5	90.2
Additional allowed regions (%)	10.1	9.1	15.5	9.0
Generously allowed regions (%)	0.2	0.0	0.0	0.8
Disallowed regions (%)	0.2	0.2	0.0	0.8

[a] Mg5/Ca45, 5 mM Mg^{2+}/45 mM Ca^{2+} (low Mg/high Ca condition); Mg2.5/Ca5, 2.5 mM Mg^{2+}/5 mM Ca^{2+} (a low Mg/low Ca condition); Mg 1.25/Ca2.5, 1.25 mM Mg^{2+}/2.5 mM Ca^{2+}; Mg5/Ca5, 5 mM Mg^{2+}/5 mM Ca^{2+} (a low Mg/low Ca condition).

[b] $R_{merge} = \sum_{hkl}\sum_{i} |I_i(hkl) - \langle I(hkl)\rangle| / \sum_{hkl}\sum_{i} I_i(hkl)$, where $\langle I(hkl)\rangle$ is the mean intensity of reflection *hkl*.

[c] $R_{factor} = \sum_{hkl} ||F_{obs}| - |F_{calc}|| / \sum_{hkl} |F_{obs}|$, where F_{obs} and F_{calc} are the observed and calculated structure factors; R_{free} is the same as the R_{factor} but is calculated for 10% of randomly selected reflections excluded from the refinement.

Table 2

The effect of Mg^{2+} on D-FFR-VIIa binding to PC/PS phospholipid bilayer

Conditions*				
Ca^{2+} mM	Mg^{2+} mM	k_{on} $M^{-1}s^{-1}$	k_{off} s^{-1}	K_d μM
1.1	0.0	1.1×10^3	3.2×10^{-3}	2.9
1.7	0.0	1.5×10^3	3.1×10^{-3}	2.1
1.1	0.6	1.9×10^3	3.2×10^{-3}	1.7

* In the presence of 5 mM Ca^{2+}, k_{on}, k_{off} and K_d values were similar to those obtained under the physiological Ca^{2+}/Mg^{2+} (1.1 mM Ca^{2+}/0.6 mM Mg^{2+}) condition (data not shown).

Table 3

The effect of Mg^{2+} on the activation of FX and FIX by FVIIa/TF assembled on the microparticles

Conditions			
Ca^{2+} mM	Mg^{2+} mM	FXa nM/min	FIXa nM/min
1.1	0.0	0.41	0.23
1.7	0.0	0.75	0.41
5.0	0.0	1.7	0.75
1.1	0.6	1.6	0.73

For these experiments,, microparticles obtained from 10^6 endotoxin stimulated monocytes were suspended in 1 ml containing 1 nM FVIIa, 100 nM FX or 100 nM ^{3}H-FIX, and varying concentrations of Ca^{2+}/Mg^{2+}. Samples were withdrawn at various time intervals and assayed for FXa or ^{3}H-FIXa activity.

Table 4

The effect of Mg^{2+} on dEGR-APC binding to PC/PS phospholipid bilayer

Conditions				
Ca^{2+} mM	**Mg^{2+} mM**	**k_{on} $M^{-1}s^{-1}$**	**k_{off} s^{-1}**	**K_d μM**
1.1	0.0	0.8×10^3	3.1×10^{-3}	3.9
1.7	0.0	3.1×10^3	3.9×10^{-3}	1.3
1.1	0.6	3.5×10^3	2.9×10^{-3}	0.8

* In the presence of 5 mM Ca^{2+}, k_{on}, k_{off} and K_d values were similar to those obtained under the physiological Ca^{2+}/Mg^{2+} (1.1 mM Ca^{2+}/0.6 mM Mg^{2+}) condition (data not shown).